Hemodynamic assessment in patients with congenital heart disease using magnetic resonance imaging

Sjöberg, Pia

2019

Document Version:
Publisher's PDF, also known as Version of record

Hemodynamic assessment in patients with congenital heart disease using magnetic resonance imaging

PIA SJÖBERG
DEPARTMENT OF CLINICAL PHYSIOLOGY | LUND UNIVERSITY

Hemodynamic assessment in patients with congenital heart disease using magnetic resonance imaging

Pia Sjöberg

LUND
UNIVERSITY

DOCTORAL DISSERTATION
by due permission of the Faculty of Medicine, Lund University, Sweden.
To be defended at Skåne University Hospital, Lund, Lecture hall 3 on Wednesday May 29 at 13:00.

Faculty opponent
Professor Philipp Beerbaum, Hannover Medical School

Organization LUND UNIVERSITY	Document name DOCTORAL DISSERTATION
	Date of issue
Author(s) Pia Sjöberg	Sponsoring organization

Title and subtitle

Hemodynamic assessment in patients with congenital heart disease using magnetic resonance imaging

Abstract

Around 1000 children are born with a heart disease in Sweden every year and today most of these children survive and reach adult age. There are around 2.3 million grownups with congenital heart disease in Europe today, a number that is expected to continue to increase. Further, the prevalence of patients with complex malformations has been growing significantly the last 10 years. There is thus a need to increase knowledge of the pathophysiology of these diseases to avoid and treat heart failure and complications, which could lead to great suffering for the patients but also great economic costs for the health care system. This thesis therefore aims to assess the cardiac function with new magnetic resonance techniques in order to increase knowledge of the pathophysiology and to better individualize treatment and optimize the timing of intervention.

The first study of this thesis investigated the ventricular kinetic energy in patients with Fontan circulation and Tetralogy of Fallot. The results showed that kinetic energy is dependent on the morphology of the heart and seems to be very specific for each individual.

In study II, III and IV the cardiac pumping in patients with Tetralogy of Fallot and pulmonary regurgitation was explored by quantifying the intraventricular kinetic energy and hemodynamic forces, as well as the atrioventricular coupling. Kinetic energy was affected in both the right and left ventricle, even if left ventricular ejection fraction was normal. Patients with pulmonary regurgitation had higher right ventricular hemodynamic forces than controls, but also affected left ventricular forces, with less alignment of force and blood flow which has been suggested to lead to pathological cardiac remodelling. Further, pulmonary regurgitation resulted in decreased right ventricular longitudinal function, decreased left ventricular preload and lower left ventricular stroke volumes. Before pulmonary valve replacement patients, similar to controls, had a clear atrioventricular coupling with a strong correlation between atrial inflow and ventricular longitudinal function. After operation however this coupling was lost, possibly because the loss of pericardial integrity.

After pulmonary valve replacement patients still had disturbed hemodynamic forces, pumping mechanics and loss of atrioventricular coupling, which is energetically unfavourable. Further studies will tell if these changes will normalize in time.

The potential role of kinetic energy and hemodynamic forces for treatment evaluation and decision making in patients with Tetralogy of Fallot can be the aim for future studies.

Key words

magneic resonance imaging, congenital heart disease, Tetralogy of Fallot, Fontan circulation, atrioventricular coupling, longitudinal function, kinetic energy, hemodynamic forces

Classification system and/or index terms (if any)

Supplementary bibliographical information		Language English
ISSN and key title 1652-8220		ISBN 978-91-7619-785-1
Recipient's notes	Number of pages	Price
	Security classification	

Hemodynamic assessment in patients with congenital heart disease using magnetic resonance imaging

Pia Sjöberg

LUND
UNIVERSITY

Evaluation committee

Associate professor Anders Ahlsson, Karolinska Institute, Sweden

Associate professor Maria Eriksson, Karolinska Institute, Sweden

Associate professor Johan Brandt, Lund University, Sweden

Thesis advisors

Associate professor Marcus Carlsson, Associate professor Erik Hedström, Associate professor Petru Liuba and Johannes Töger, PhD

Faculty of Medicine
Department of Clinical Physiology

ISBN 978-91-7619-785-1
ISSN 1652-8220

Printed in Sweden by Media-Tryck, Lund University
Lund 2019

“Wonder is the beginning of wisdom.”

— *Socrates*

Table of Contents

List of publications

This thesis is based on the following papers which in the text will be referred to by their Roman numbers.

I. Decreased Diastolic Ventricular Kinetic Energy in Young Patients with Fontan Circulation Demonstrated by Four-Dimensional Cardiac Magnetic Resonance Imaging. *Pediatr Cardiology.* 2017; 38:669-680

II. Disturbed left and right ventricular kinetic energy in patients with repaired tetralogy of Fallot: pathophysiological insights using 4D-flow MRI. *Eur Radiol.* 2018; Oct;28(10):4066-4076

III. Altered biventricular hemodynamic forces in patients with repaired tetralogy of Fallot and right ventricular volume overload because of pulmonary regurgitation. *Am J Physiol Heart Circ Physiol.* 2018; 315: H1691-H1702

IV. Changes in left and right ventricular longitudinal function after pulmonary valve replacement in patients with Tetralogy of Fallot. (Manuscript)

Author's contributions

	Study design	Ethical application	Data collection	Data analysis	Statistics	Figures/Tables	Interpretation of results	Preparation of manuscript	Revision of manuscript	Reply to reviewers
Study I	2	0	3	3	2	3	3	3	3	3
Study II	3	3	3	3	3	3	3	3	3	3
Study III	3	3	3	3	3	3	3	3	3	3
Study IV	3	3	3	3	3	3	3	3	-	-

Not applicable
No contribution 0
Limited contribution 1
Moderate contribution 2
Significant contribution 3

Summary

Around 1000 children are born with a heart disease in Sweden every year and today most of these children survive and reach adult age. There are around 2.3 million grownups with congenital heart disease in Europe today, a number that is expected to continue to increase. Further, the prevalence of patients with complex malformations has been growing significantly the last 10 years. There is thus a need to increase knowledge of the pathophysiology of these diseases to avoid and treat heart failure and complications, which could lead to great suffering for the patients but also great economic costs for the health care system. This thesis therefore aims to assess the cardiac function with new magnetic resonance techniques in order to increase knowledge of the pathophysiology and to better individualize treatment and optimize the timing of intervention.

The first study of this thesis investigated the ventricular kinetic energy in patients with Fontan circulation and Tetralogy of Fallot. The results showed that kinetic energy is dependent on the morphology of the heart and seems to be very specific for each individual. Further studies will tell if changes in kinetic energy will provide early information on ventricular dysfunction or development of aortopulmonary collaterals.

In study II, III and IV the cardiac pumping in patients with Tetralogy of Fallot and pulmonary regurgitation was explored by quantifying the intraventricular kinetic energy and hemodynamic forces, as well as the atrioventricular coupling. Kinetic energy was affected in both the right and left ventricle, even if left ventricular ejection fraction was normal. Patients with pulmonary regurgitation had higher right ventricular hemodynamic forces than controls, but also affected left ventricular forces, with less alignment of force and main blood flow directions which has been suggested to lead to pathological cardiac remodelling. Further, pulmonary regurgitation resulted in decreased right ventricular longitudinal function, decreased left ventricular preload and lower left ventricular stroke volume. Before pulmonary valve replacement patients, similar to controls, had a clear atrioventricular coupling with a strong correlation between atrial inflow and ventricular longitudinal function. After operation however this coupling was lost, possibly because the loss of pericardial integrity.

The potential role of kinetic energy and hemodynamic forces for treatment evaluation and decision making in congenital heart disease and the long-term effect of surgery on atrioventricular coupling can be the aim for future studies.

Populärvetenskaplig sammanfattning

I Sverige föds det ca 1000 barn varje år med medfött hjärtfel. Symtomen varierar mycket allt från dem som inte behöver någon behandling till dem som behöver akut behandling redan vid födelsen och fortsatt under resten av livet. För att bättre kunna vägleda behandlingen och även kunna utvärdera den behövs bättre förståelse av det sjuka hjärtats funktion.

Fallots tetrad är ett hjärtfel som orsakar att icke syresatt blod passerar genom ett hål i kammarskiljeväggen och ut i kroppen pga att det är trångt i utflödet till lungcirkulationen. Hjärtfelet opereras oftast inom det första halvåret, men efteråt uppstår det ofta ett läckage i lungpulsåderklaffen, vilket gör att höger kammare belastas med större blodvolymer än vanligt och därför blir större.

En del barn föds med mycket komplexa hjärtfel som man inte kan korrigera så att det blir två fungerande kamrar. Dessa patienter opereras i olika steg där slutsteget är att en kammare pumpar runt blodet i kroppen och att blodet passivt dräneras till lungcirkulationen. Denna typ av cirkulation kallas för Fontancirkulation.

Magnetresonans ger möjlighet att tidsupplöst kunna studera hjärtats volymer och flöden. Genom att mäta flödet fyrdimensionellt, får man hastigheten av blodet i alla tre dimensioner i rummet samt över tid. Utifrån dessa värden kan rörelseenergin och kraftutbytet mellan blod och hjärtmuskel kvantifieras.

Syftet med avhandlingen var att studera hjärtfunktionen hos patienter med Fontancirkulation och Fallots tetrad med hjälp av magnetresonans (MR) för att bättre förstå fysiologin och därmed kunna utveckla nya metoder för att kunna vägleda och utvärdera behandling.

Delarbete I visade att rörelseenergin i hjärtat hos patienter med Fontanscirkulation är beroende av morfologin av kammaren, dvs om det är en höger- eller vänsterkammare, och att rörelseenergin under hjärtcykeln verkar vara specifik för varje individ. Förändringar i hjärtats rörelseenergi skulle kunna ge tidig information om nedsatt hjärtfunktion eller utveckling av kollateralkärl mellan kroppspulsådern och lungkärlen.

Delarbete II visade att rörelseenergin hos patienter med Fallots tetrad och läckage i lungpulsåderklaffen är förhöjd i höger kammare under diastole, den period då kammaren fylls med blod. Rörelseenergin under hjärtcykeln verkar också avspegla huruvida höger kammare är restriktiv eller inte. I vänster kammare, där funktionen bedömts som normal med konventionella metoder, visade sig rörelseenergin vara nedsatt under systole, den period då kammaren pumpar ut blod. Efter operation av lungpulsåderklaffen så sjönk rörelseenergin i höger kammare, men var fortfarande nedsatt i vänster kammare.

Delarbete III undersökte hur kraftutbytet mellan blod och hjärtmuskel ser ut hos patienter med Fallots tetrad och läckage i lungpulsåderklaffen. I vänster kammare var krafterna i mindre utsträckning riktade i flödesriktningen av blodet, vilket inte är optimalt ur energisynpunkt. I höger kammare sågs ökade krafter längs med inflödet från förmak och lungpulsåder. Efter operation av lungpulsåderklaffen kvarstår förändringar i båda kamrar, vilket talar för att hjärtats sätt att pumpa inte har blivit normalt.

Delarbete IV visade hur kopplingen mellan förmak och kammare fungerar hos patienter med Fallots tetrad och läckage i lungpulsåderklaffen före och efter utbyte av klaff. Det längsgående bidraget till funktionen är nedsatt i höger kammare bla pga den ökade volymen från klaffläckaget, men det minskar ytterligare efter operation. Läckaget gör också att vänster förmak fylls sämre och vänster kammare får mindre blodvolym att pumpa med, men det längsgående bidraget till vänster kammares funktion är inte påverkad. Efter operation av klaffen försämras kopplingen mellan förmak och kammare, sannolikt pga att hjärtsäcken har öppnats under operationen.

Abbreviations

2D:	two dimensional
4D:	four dimensional
Ao:	aorta
AV-plane:	atrioventricular plane
APC:	aortopulmonary collaterals
ASD:	Atrial septal defect
AVPD:	atrioventricular plane displacement
AVSD:	atrioventricular septal defect
BSA:	body surface area
CMR:	cardiac magnetic resonance
CoA:	Coarctatio of aorta
DILV:	Double inlet left ventricle
DORV:	Double outlet right ventricle
ECG:	electrocardiogram
EDV:	end-diastolic volume
f:	force
g:	pressure gradient
HLHS:	Hypoplastic left heart syndrome
IVC:	inferior vena cava
KE:	kinetic energy
LCS:	lagrangian coherent structures
LPA:	left pulmonary artery
LA:	left atrium
LV:	left ventricle
LVOT:	left ventricular outflow tract
m:	mass
MAPCA:	major aortopulmonary collateral arteries
MAPSE:	mitral plane excursion

MRI:	magnetic resonance imaging
NYHA:	New York Heart Association Functional Classification
N, n:	number
ρ:	density
PLE:	Protein-losing enteropathy
PS:	pulmonary stenosis
PVR:	pulmonary valve replacement
ToF:	Tetralogy of Fallot
TGA:	Transposition of the great arteries
RA:	right atrium
rToF:	repaired Tetralogy of Fallot
RMS:	root mean square
RV:	right ventricle
RVOT:	right ventricular outflow tract
SVC:	superior vena cava
SV:	stroke volume
TAPVD:	Total Anomalous Pulmonary Venous Drainage
TAPSE:	tricuspid plane excursion
VSD:	ventricular septal defect
v:	velocity
VO_2:	peak: peak oxygen uptake
μ:	viscosity

1 Introduction

Every year about 1 000 children are born with a heart defect in Sweden.[1–3] The severity of the condition varies a lot. Some conditions hardly need any treatment, however some must be treated immediately after birth. Today about 98% of children with congenital heart defects will reach adult age.[4,5]. In Sweden there are around 40 000 grown-ups with congenital heart defects, while in Europe the estimate is 2.3 million, numbers that are expected to continue to increase.[6,7] Further, due to improved treatment, the prevalence of patients surviving with complex malformations have been growing significantly the last 10 years.[8]

There are guidelines for management of patients with congenital heart disease,[9,10] but there is a lack of strong evidence to support them. Most of the recommendations are based on expert opinions, case studies and standard of care. Further, many larger studies of congenital heart disease are descriptive or observational with blunt endpoints like death and arrhythmias. Research related to Tetralogy of Fallot and patients with single ventricle and Fontan circulation has recently been addressed as a top priority.[11] To get better functional measurements to guide therapy and evaluate results after treatment more knowledge about the pathophysiology is crucial.

1.1 The healthy heart

The heart is a pump with the purpose to deliver enough volume per minute as the metabolism in the body requires. In an adult person this amounts to approximately 70 ml of blood per heartbeat, which is called stroke volume, or 5 liters per minute, which is called cardiac output. [12] The heart is constructed in an ingenious way to do this with a minimal dissipation of energy.

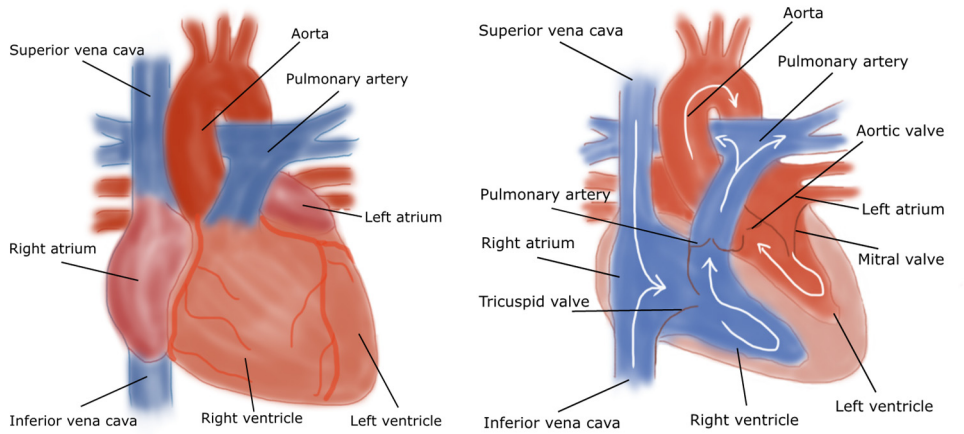

Figure 1.1 The heart and the great vessels
Blue colour indicates blood low on oxygen and red colour blood high on oxygen. White arrows show the flow direction of the blood.

The heart has four chambers; two atria and two ventricles (Figure 1.1). The ventricles are divided by a muscular wall, called the septum. Between the atria and the ventricles is the atrioventricular plane (AV-plane), with the tricuspid valve separating the atrium and the ventricle on the right side and the mitral valve separating them on the left. The left ventricle is conical shaped with the in- and outflow tract at the same end. In contrast, the right ventricle is crescent-shaped with the inflow approximately parallel to the left ventricular inflow, but the right ventricular outflow crossing over the left ventricular outflow tract.

The heart receives blood from the body through the superior and inferior caval veins. The venous blood, low on oxygen, enters the right atrium and then passes through the tricuspid valve to the right ventricle. The right ventricle ejects the blood to the pulmonary trunk via the pulmonary valve. The oxygenated blood returns from the lungs to the heart via the pulmonary veins to the left atrium and then via the mitral valve to the left ventricle. Finally, the left ventricle ejects the blood to the body through the aortic valve.

The pressure in the pulmonary circulation is approximately one fifth of the pressure in the systemic circulation which is why the right ventricle does not have to generate as much pressure compared to the left to eject the same amount of blood.[12]. Therefore, the right ventricle is thin-walled structure compared to the left ventricle which has much thicker muscle wall or myocardium.

1.2 Cardiac pumping

The heart is enclosed in the pericardium, a double-layered membrane less than one mm thick with a parietal layer made of tough fibrous tissue.[13] The volume of the pericardial sack is almost constant during the cardiac cycle, which also entails that the heart inside only varies 5-8% in volume over a heartbeat.[14,15]

When the heart pumps it works like a piston pump with the as piston and the ventricles as cylinders.[14,16] When the ventricles contract, they will pull the AV-plane towards the apex of the heart and eject their content to the lungs or body respectively. Almost simultaneously, since the volume of the heart is nearly constant, there will be a pressure drop in the atria that will cause blood to get sucked in to the atria which will expand. If the heart worked like a complete constant-volume pump it would have been more efficient since energy is lost when tissues must be moved. However, the total heart volume decreases during ventricular contraction (systole) when the heart ejects more blood from the ventricles than fills the atria. During diastole when the ventricular muscle recoil and the ventricle aspirates blood in from the atria the volume gets restored. The total heart volume variation during the cardiac cycle has been shown to mainly be caused by radial pumping [17]. The longitudinal pumping caused by the displacement of the AV-plane contributes to approximately 80% of the right ventricular stroke volume and the radial movement of the lateral wall contributes to 20%.[17] In the left ventricle longitudinal contribution to stroke volume is about 60% and the radial movement of the septum and lateral wall contributes to 40%.

The looped shape of the heart has been proposed to facilitate the bloods path, so it conserves as much energy as possible.[18] The positions of the veins and the looped arrangement of the heart cause a forward rotational flow of the blood entering the atria during ventricular contraction. This keeps the momentum of the blood and redirects the flow towards the atrioventricular valve. When blood, during diastole, passes the AV-valves a vortex ring is created recirculating the flow and facilitating the rerouting of the flow toward the outflow tract (Figure 1.2).

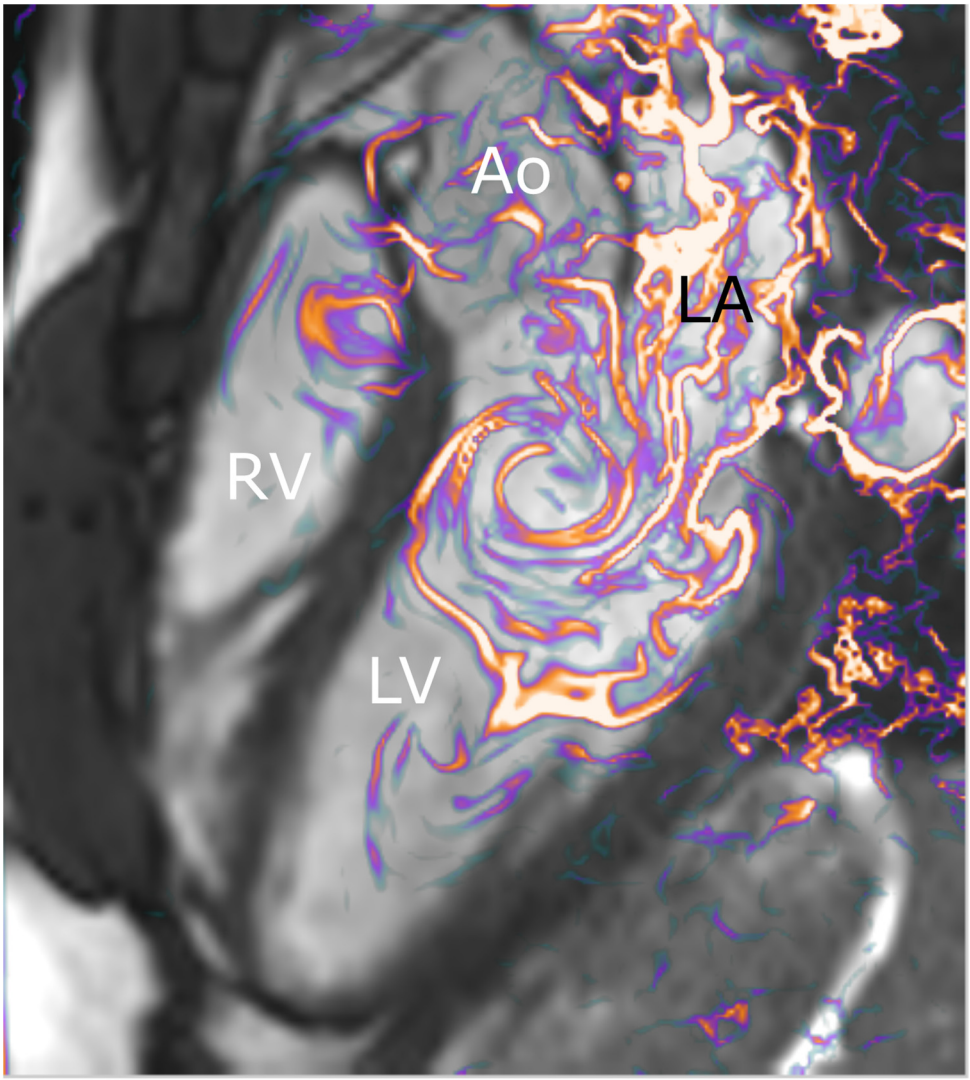

Figure 1.2 Vortex formation in the left ventricle
When blood during diastole passes the AV-valves a vortex ring is created recirculating the flow and facilitating the rerouting of the flow toward the outflow tract. RV, right ventricle; LV, left ventricle; RA, right atrium; LA, left atrium; Ao, Aorta.

1.3 Tetralogy of Fallot

Tetralogy of Fallot (ToF) is the most common cyanotic congenital heart defect and a recent study from Germany showed that ToF constitutes for approximately 9% of all congenital heart defects.[2,8]

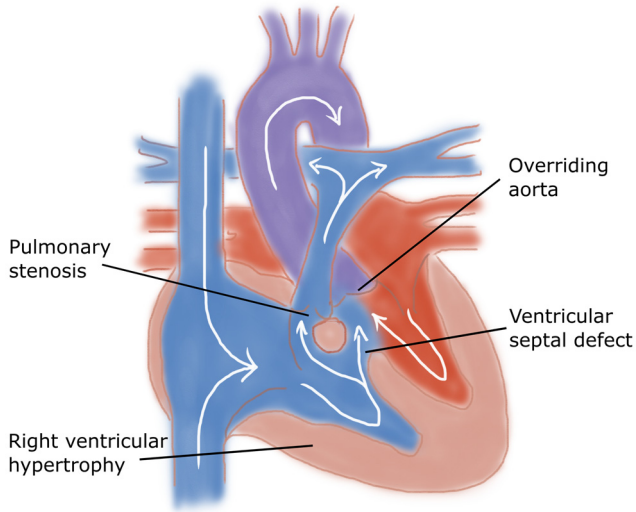

Figure 1.2 Tetralogy of Fallot
Tetralogy of Fallot with pulmonary stenosis, ventricular septal defect (VSD), overriding aorta and hypertrophy of the right ventricle. Deoxygenated blood will pass through the VSD to the left side of the heart because of the obstruction of the right ventricular outflow tract and pulmonary stenosis.

ToF consists of four criteria, pulmonary stenosis, ventricular septal defect (VSD), overriding aorta and hypertrophy of the right ventricle (Figure 1.2). The clinical manifestation with cyanosis is most commonly shortly after birth, although the number of patients diagnosed prenatally is growing.[19] The cyanosis is caused by desaturated blood entering the systemic circulation through the large VSD, instead of passing through the pulmonary valve to the lungs. If the pulmonary stenosis is severe the patients' pulmonary circulation might be dependent on a patent arterial duct or a surgically created shunt if repair is not performed. The repair consists of closure of the VSD with a patch, relieving the pulmonary stenosis by infundibular resection and opening the pulmonary valve by commissurotomy (Figure 1.3). Sometimes the annulus of the valve is too small and a transannular patch is required, which increases the risk of severe pulmonary regurgitation.

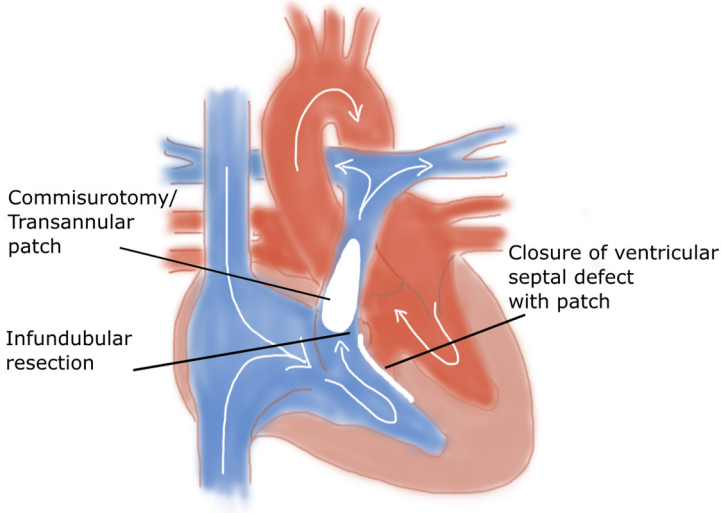

Figure 1.3 Repair of Tetralogy of Fallot
Repair of Tetralogy of Fallot includes closure of the ventricular septal defect with a patch, infundibular resection and commissurotomy. Sometimes a transannular patch is needed.

In the early days of cardiac surgery, the mortality in connection with repair was very high. This led to development of the two-stage repair with a shunt first and repair later, which was more successful.[20] Gradually over the years, improved surgical techniques and perioperative care reduced the operative mortality and today mortality for primary repair is less than 1% in Sweden.[19] Patients can now be operated earlier, thereby reducing the effects of cyanosis and avoiding development of right ventricular hypertrophy. Today it is even possible to do neonatal repairs if needed, but the risk of transannular patch is then higher.[21,22]

It's important to follow patients with ToF to evaluate the degree of pulmonary regurgitation which might cause ventricular dilatation, decreased exercise capacity, ventricular arrhythmias and sudden death(Figure 1.4).[10,23,24] The dilemma is however to decide the optimal time for pulmonary valve replacement (PVR).[25–28] The benefit of an operation must overweigh the risks. The overall survival after PVR has been shown to be 97% at 1 year and 92% at 10 years after PVR.[29] After PVR the risk for valve failure was around 7-20% after 5 years, 30-40% after 10 years and 60% after 15 years in earlier studies but a more recent study shows the need of reintervention of 2% after 5 years and 4% after 10 years, indicating clear improvement of the long-term results.[29–31] However, even if right ventricular volumes decrease initially after PVR, the volumes gradually return to the values similar to those before PVR at 7 to 10 years after PVR.[32] Further, there will still remain an increased risk of arrythmia and mortality after PVR.[33,34] Commonly

reported thresholds for right ventricular volumes above which normalization of volumes after PVR are unlikely have been 70-80 ml/m^2 for end-systolic volume and 150-160 ml/m^2 for end-diastolic volume.[25,35] According to European Society of Cardiology Guidelines, PVR should be considered in patients with severe pulmonary regurgitation if they are symptomatic or if they have decreased exercise capacity, progressive right ventricular dilatation, progressive right ventricular dysfunction, progressive tricuspid regurgitation or arrhythmias.[10] In summary, there are still concerns about the benefit of PVR and finding the right balance between the risk of irreversible damage to the right ventricle and risk for repeated reinterventions after PVR.[36]

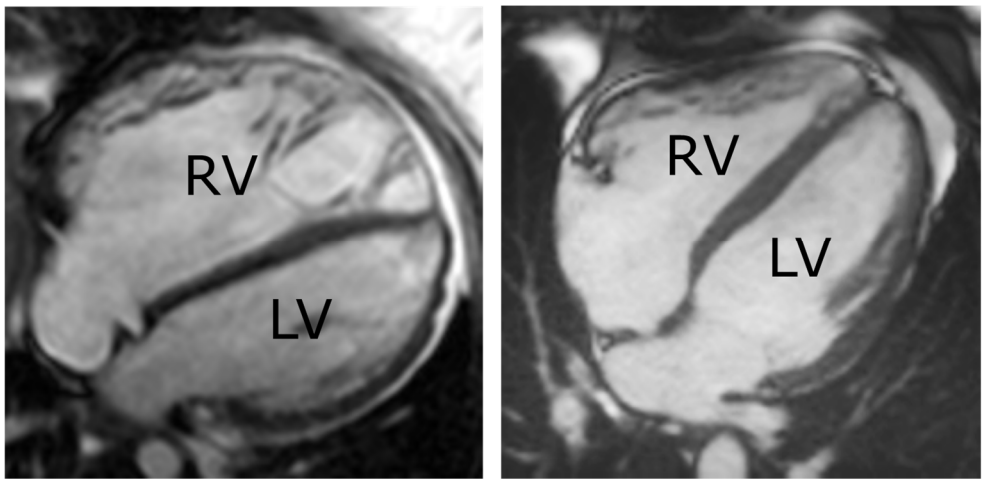

Figure 1.4 Dilatation of the right ventricle
Four chamber magnetic resonance image showing to the left a dilated right ventricle (RV) caused by pulmonary regurgitation. Right panel shows a normal-sized right ventricle with equal-sized left ventricle (LV).

The encouraging fact that most children with ToF will reach adulthood stresses the importance of understanding the pathophysiology not only to avoid complications for the adult patients, but also to be able to further improve the treatment of the young child with this malformation.

1.3 Fontan circulation

Some patients are born with complex cardiac malformations that cannot be repaired in such a way that the result will be two ventricles, one pumping to the systemic circulation and one to the pulmonary circulation. Pfitzer *et al* found that 9% of all patients with congenital heart defects in Germany has a univentricular heart.[8] These patients can have various forms of malformations, but all have a single-ventricle physiology. The morphology of the single ventricle can be either right or left. Patients have complete mixing of the arterial and venous blood and are dependent on an open arterial duct to be able to circulate blood to both the body and lungs.

The treatment for patients with single-ventricle physiology has continuously developed since the late 1970s and nowadays most patients reach adult age.[37] Today, depending on the type of malformation, a first operation is performed in the neonatal period. This operation results in a single common ventricle with one major blood vessel to the body. To provide the lungs with blood a Gore-Tex graft is inserted between a branch of the aorta and a branch of the pulmonary artery (Blalock-Taussig shunt) or between the ventricle and the pulmonary artery (Sano-shunt). When patients reach 4-6 months of age the superior caval vein is connected directly to the right pulmonary artery branch, a so-called bidirectional Glenn (Figure 1.3). At the same time the shunt is closed.

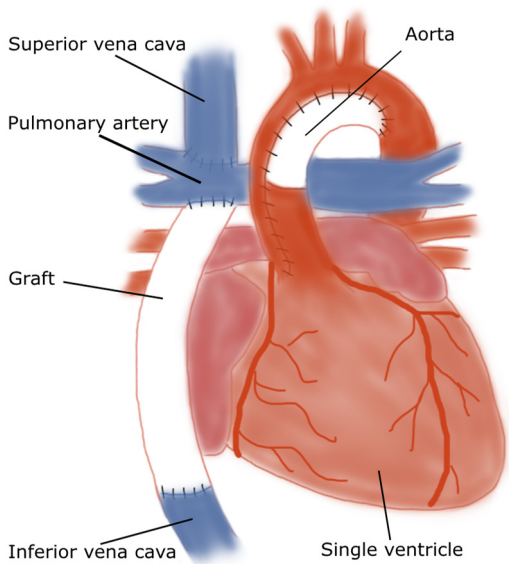

Figure 1.3 Fontan circulation
Fontan circulation with the superior caval vein and the inferior caval vein via a Gore-Tex© graft direct connected to the pulmonary artery.

To get the patient fully saturated all venous blood must drain to the pulmonary circulation and this is achieved by also connecting the inferior vena cava to the pulmonary artery. Initially, as described by Dr Fontan in 1971, this was performed by isolating the right atrium from the rest of the heart and connecting the atrial appendage to the pulmonary artery.[38] This, unfortunately, led to dilatation of the right atrium with arrhythmias and blood clotting.[39,40] To avoid this problem a lateral tunnel inside the right atrium was created to direct the blood from the inferior caval vein to the pulmonary artery.[41–43] Nowadays the most common way of performing a Fontan operation is to connect Gore-Tex graft from the inferior caval vein to the pulmonary artery outside the heart, an operation that has less problems with atrial arrythmias postoperatively (Figure 1.3).[37,44–46] Today a Fontan operation is commonly performed at 18-24 months of age.

Survival rates 15 years after operation have been reported as 81-95%, but a decline in survival is noted after 20-25 years.[47–50] Technical developments have led to long-term prognoses improving over the years and time will tell how this will affect the survival rates.

The Fontan circulation depends on a good heart function, both systolic and diastolic, good valve function and low resistance in the pulmonary circulation. Patients will have higher venous pressure than normal which drives the blood forward, but also the skeletal-muscle pumping function and inspiration will assist the blood flow to the lungs.

However, even when patients have preserved ventricular contraction, they will suffer from preload deprivation, i.e. too little blood to fill the ventricle, and thereby low cardiac output.[51] The low preload results in the inability of the ventricle to increase cardiac output by increasing systolic contractility and thus also the possibility to increase the flow to the pulmonary circulation. It is therefore utterly important to avoid any restriction of the flow in the Fontan pathway, since this would cause a decrease in ventricular preload and increased venous congestion. In time the chronic venous hypertension can cause complications like thromboembolism, protein-losing enteropathy, plastic bronchitis or liver failure.[52] Small changes in the circulation could be of great importance but with the methods commonly used to monitor these patients today it is difficult to detect them. It is therefore of interest to find new methods to detect these changes early but also important to learn more about the pathophysiology to be able to properly interpret the results.

1.4 Kinetic energy

To accelerate an object a force must be applied, which requires work. Energy is transferred to the object that will be moving at a constant speed if no new force is applied. The transferred energy, called kinetic energy, depends on the mass and velocity of the object and is calculated as $KE=\frac{1}{2}mv^2$. In the heart the myocardium applies a force on the blood to accelerate it and thus, the better the kinetic energy is preserved the less work the heart must do.

Intraventricular kinetic energy can be quantified using MRI.[53] The kinetic energy is higher in the right ventricle during ventricular contraction compared to the left ventricle. The long outflow tract in the right ventricle gives rise to higher velocities than in the short left ventricular outflow tract. During diastole kinetic energy reflects the pumping mechanics of the heart with left ventricular recoil causing blood to get aspirated into the ventricle to a higher extent than in the right ventricle with higher kinetic energy as a result. In contrast, in the right ventricle where 80% of the function is caused by longitudinal pumping compared to 60% in the left, the diastolic peak kinetic energy is lower. Movement of the AV-plane toward the base of the heart incorporating blood in the atrium does not cause much rise in kinetic energy.

At rest kinetic energy contributes very little to the total work of the heart, but at exercise it becomes much more important.[53–55] Intraventricular kinetic energy has also shown to be different in patients with heart failure, cardiomyopathy and mitral regurgitation compared to healthy volunteers and might improve the understanding of the hemodynamics in patients with congenital heart disease.[56–58]

1.5 Hemodynamic forces

The rerouting of flow in the heart depends on forces of the myocardium changing the direction of the blood. A force has a magnitude and a direction and can be measured as intraventricular pressure gradients. To make them easier to interpret they can be integrated to a vector force reflecting the global net force between the blood and the myocardium. Similar to kinetic energy hemodynamic forces reflect how the heart pumps and have been shown to be very consistent in healthy volunteers and athletes but disturbed in patients with cardiomyopathy and left bundle branch block.[59–61] Misalignment of forces and the main flow directions in the heart would theoretically waste energy, but studies also suggest that it would lead to pathological cardiac remodelling, which is why this measurement is of interest in congenital heart disease.[62]

1.6 Magnetic Resonance Imaging

Magnetic Resonance Imaging (MRI) can be used to obtain images of the body in any given plane. It is a non-invasive and non-ionizing technique which is therefore suitable for repeated examinations.

The MR imaging process uses hydrogen atoms in the human body to generate the signals and images. The human body is approximately 70% made of water. Each water molecule contains two hydrogen atoms with one proton each. These protons work like small magnets spinning around the magnetic axis at a certain resonance frequency, called the Larmor frequency. The hydrogen protons in the body points in different directions but just like a compass needle wants to line up with the magnetic poles of the earth, the hydrogen protons of the body line up if put into a strong external magnetic field such as a MR scanner.

By transmitting a radio frequency pulse which matches the Larmor frequency, the protons absorb the energy and flip. This is called resonance. After the pulse ends the protons continues to precess and gradually realign with the external magnetic field at a speed depending on what tissue the water is in. This will release energy which is detected by the scanner.

The scanner measures the time for the protons to relax in two ways; T1 which is the time for the magnetic vector to return to 63% of its resting state and T2 which is the time it takes for the axial spin to have 37% of its original magnitude. By monitoring the different relaxation times and programming the scanner to send out the radio frequency pulse in different ways, different tissues can be distinguished.

To be able to locate the MRI signal to different parts of the body, the magnetic field can be varied in different parts of the body with so-called gradient magnets. By applying a gradient, the magnetic field varies in strength, so that protons at different positions will precess and resonate at different frequencies. This is called magnetic field gradient and enables the scanner to find where in the body a certain tissue is.

The signals detected by the scanner are put together to a k-space, which is a collection of numbers representing the spatial frequencies in a MR image. The k-space is finally converted into an image by a mathematical procedure called the Fourier transform.

Motion makes MRI more challenging. When imaging the heart patients are often asked to hold their breath to compensate for respiration, but compensation for cardiac intrinsic motion requires more technical solutions. By monitoring the electrocardiogram (ECG) the scanner can detect the R-wave on the ECG and synchronize the acquisition. ECG-synchronized images can be produced as movies of the pumping motion of the heart and blood flow, so-called “cine” imaging.

To measure blood flow the scanner uses the changes of magnetisation in the blood moving in the same direction as the magnetic field gradient, a technique called phase contrast. Depending on how far the protons have moved, i.e. their velocities, since the radio frequency pulse was applied, they will have different phase shifts due to the gradient field. By applying a biphasic (balanced) gradient the static tissue will return to a net zero phase shift and the protons in the blood will have different phase shifts, depending on the direction.

Flow is most often measured in one plane or two dimensions. However, if the velocities in each voxel is encoded in three dimensions and if repeated in consecutive slices it enables flow measurements in three dimensions of larger volume, like the whole heart. If this information is combined with temporal information, it is called four-dimensional phase contrast imaging. This technique offers a unique possibility to retrospectively visualise and quantify blood flow in all regions over the whole cardiac cycle. It enables for example quantification of flow volume, velocity, kinetic energy and pressure gradients.

1.7 Exercise testing with gas analysis

Exercise testing is commonly used to evaluate the cardio-respiratory function. Exercise with gradually increasing workload on a stationary bicycle ergometer is most common in Sweden. To assess the cardiac response blood pressure, heart rate, ECG and symptoms are monitored during the examination and measurements of the oxygen saturation of the blood can also be performed.

The ability to perform exercise is related to the cardiovascular and respiratory systems capacity to deliver oxygen to the muscles and clear the blood of carbon dioxid. This process includes four parts; 1. Pulmonary ventilation - air going in and out of the lungs; 2. Pulmonary diffusion – exchange of oxygen and carbon dioxid between lungs and blood; 3. Transportation of oxygen to the tissues and carbon dioxid to the lungs; 4. Capillary gas exchange between blood and muscle.

During exercise the muscles will need more oxygen and by adding gas exchange analysis to the exercise test the cardiovascular and respiratory systems' capacities can be tested in more detail. The patients will be wearing a facemask covering mouth and nose and inspired oxygen and expired carbon dioxid can be continuously measured during exercise.

One of the analysed parameters is peak VO_2, which is the highest rate of oxygen uptake reached during the examination. Peak VO_2 reflects the maximal ability to deliver oxygen to the tissues and thereby the exercise capacity.

2 Aims

The aim of the thesis was to assess the cardiac function with new magnetic resonance techniques in patients with 1) repaired Tetralogy of Fallot and pulmonary regurgitation and 2) patients with single ventricles and Fontan circulation. The purpose was to increase knowledge of the pathophysiology to better individualize treatment and optimize the timing of interventions.

The specific aims of each paper were:

I. to non-invasively quantify the kinetic energy during the entire cardiac cycle of the single ventricle in Fontan patients using four-dimensional phase-contrast magnetic resonance imaging to better understand the circulation and the pathophysiology of complications.

II. to evaluate ventricular kinetic energy during the entire cardiac cycle in patients with repaired Tetralogy of Fallot with moderate or severe pulmonary regurgitation compared to controls, in order to describe the pathophysiological effects of pulmonary regurgitation on the left and the right ventricles.

III. to quantify the hemodynamic forces in the right and left ventricle to further understand the pathophysiological mechanisms in patients with repaired Tetralogy of Fallot and right ventricular volume overload because of pulmonary regurgitation.

IV. to investigate atrioventricular coupling as well as interventricular interaction before and after surgical pulmonary valve replacement to better understand the pumping mechanism in repaired Tetralogy of Fallot with pulmonary regurgitation.

What we observe is not nature itself, but nature exposed to our method of questioning.

— Werner Heisenberg

3 Material and Methods

3.1 Study Population

Study I

Eleven patients with Fontan circulation referred to cardiovascular magnetic resonance examination were prospectively included. Five patients were below 10 years of age and were examined under general anaesthesia. Patients' characteristics are described in table 1.

Patients' clinical status were evaluated by their treating pediatric cardiologist. Five patients were clinically stable, and 6 patients had various complications, defined as the need of intervention in the Fontan circulation. Aortopulmonary collaterals were evaluated during catheterization using fluoroscopic angiography of the thoracic aorta and the degree of collateral flow was assessed by MRI. Blood flow in the aortopulmonary collaterals was calculated using MRI by subtracting the flow volume in the caval veins from the aortic flow measured by two-dimensional (2D) flow. The difference between pulmonary and caval venous flows was used for aortopulmonary collateral quantification in three patients where aortic flow measurements were not available.[63] Seven of the 11 patients underwent catheterization as part of the clinical evaluation. Hemodynamically significant aortopulmonary collaterals were defined as enlarged aortopulmonary collaterals with saturation step-up in the pulmonary artery branches in combination with elevated end-diastolic pressure (measured by catheterization) and >25% aortopulmonary collateral flow contribution to stroke volume.

Six patients had complications with need of intervention for pulmonary branch stenosis in four cases, restrictive atrial communication in one case and severe aortopulmonary collaterals in one case. Three patients underwent a follow-up MRI after surgical or percutaneous intervention.

Eight healthy volunteers (2 females, median age 26 years, range 23–36) with blood pressure <140/90, normal ECG, no cardiovascular medication, and no medical history of cardiovascular or other systemic disease were used as controls.

Table 1.
Patients' characteristics

Subject	Age at time of CMR (y)	Sex	BSA (m^2)	Ventricular morphology	Type of Fontan	Diagnosis	APC	Complications	NYHA
1	3	M	0.56	Left	Extracardiac	Unbalanced AVSD, small LV, PA, MAPCA, right isomerism, bilateral SVC, dextrocardia. Fenestrated*	*	PLE	II
2	7	M	0.82	Left	Extracardiac	HLHS, borderline	yes	Restrictive ASD	III
3	4	M	0.68	Right	Extracardiac	HLHS, TAPVD, bilateral SVC	yes	PLE	IV
4	12	F	1.26	Right	Extracardiac	Hypoplastic right PA, left isomerism, interrupted IVC, dextrocardia	no	Pulmonary arteriovenous fistulas	IV
5	4	M	0.72	Right	Extracardiac	Hypoplastic aortic arch, CoA, VSD, DORV	yes	LPA stenosis	II
6	15	M	1.60	Right	Extracardiac	DORV Taussig Bing, unbalanced AVSD, PS, TAPVD, right isomerism	yes	APC	II
7	17	M	1.72	Right	Lateral tunnel	Single ventricle, DORV, TGA, dextrocardia	no	no	I
8	14	F	1.37	Right	Extracardiac	Single ventricle, PS, TGA, right isomerism, bilateral SVC, TAPVD	yes	no	I
9	13	F	1.36	Left	Extracardiac	TGA, multiple VSD, hypoplastic pulm arteries	yes	no	I
10	29	M	1.72	Left	Right atrium to PA	Tricuspid atresia	no	no	I
11	4	M	0.72	Left with long outflow tract	Extracardiac	DILV, TGA, PS, left pulm artery stenosis	no	no	II

CMR, Cardiac Magnetic Resonance; BSA, body surface area; APC, aortopulmonary collaterals; NYHA, New York Heart Association Functional Classification; AVSD, atrioventricular septal defect; LV, left ventricle; MAPCA, major aortopulmonary collateral arteries; SVC, superior vena cava; HLHS, Hypoplastic left heart syndrome; TAPVD, Total Anomalous Pulmonary Venous Drainage; IVC, inferior vena cava; CoA, Coarctatio of aorta; VSD, ventricular septal defect; DORV, Double outlet right ventricle; PS, pulmonary stenosis; TGA, Transposition of the great arteries; DILV, Double inlet left ventricle; PLE, Protein-losing enteropathy; ASD, Atrial septal defect; LPA, left pulmonary artery. * Fenestrated extracardiac tunnel which makes the assessment of APC difficult.

Study II

Fifteen patients with repaired Tetralogy of Fallot (rToF), 5 women and 10 men, referred for cardiovascular MRI were prospectively included. Patients were between 18 and 52 years old, median age 24 years, and had pulmonary regurgitation between 21 and 54%, mean 39±9%, but no pulmonary stenosis. Seven of the patients had a systemic to pulmonary shunt prior to the corrective surgery which was performed at a median age of 14 months, ranging from 2 months to 29 years. Ten patients had repair with transannular patch. Time from corrective surgery to examination was between 18 and 46 years. One patient underwent pulmonary valve replacement (PVR) and one had stenting of a pulmonary branch stenosis between primary corrective surgery and inclusion in the study. Six of the patients underwent PVR after study inclusion and had a follow-up MRI 6–12 months after operation with the same protocol as baseline. Indications for PVR were pulmonary regurgitation fraction ≥35%, progressive right ventricular dilatation with end-diastolic volume ≥150 ml/m2 and/or symptoms and signs of heart failure. Fourteen healthy volunteers, two women and 12 men, mean age 30±7 years, were used as controls for comparison.

Study III

Eighteen patients, 11 men and 7 women, of which 15 was also included in study II were prospectively included. Mean age was 29±13 years. Two of the three added patients had systemic to pulmonary shunt prior to the corrective surgery. They had their primary correction between the age of 11 months to 10 years. One of the three patients had resection of subvalvular pulmonary stenosis and a valvotomy between primary correction and inclusion in the study. Fifteen healthy controls, 5 women and 10 men, mean age 31±7 years, were used as controls.

Study IV

Twelve patients with repaired ToF, mean age 37±13 years, ten of them also included in study III, with pulmonary regurgitation >35% (mean 44±6%), no pulmonary stenosis, progressive right ventricular dilatation with end-diastolic volume ≥150 ml/m^2 and/or symptoms and signs of heart failure were prospectively included. Four of the patients had systemic to pulmonary shunt prior to the corrective surgery. Age at correction was between 3 months and 29 years. One patient had stenting of a pulmonary branch stenosis and one had PVR between primary corrective surgery and examination. All patients had surgical PVR performed and had re-examination within 6-12 months after. Fifteen healthy controls, 5 women and 10 men, mean age 31±7 years, were used as controls.

3.2 Image Acquisition

MRI was performed with ECG retrospective gating using a either a 1.5 T Achieva (Philips Healthcare, Best, the Netherlands) or a 1.5 T Magnetom Aera (Siemens Healthcare, Erlangen, Germany). Patients were examined with the same scanner before and after PVR. A steady-state balanced free precession sequence was used to collect cine images covering the entire heart in short and long-axis views. Two-dimensional flow measurements in the aorta and pulmonary artery were acquired during free breathing by a phase-contrast velocity-encoding. Three-dimensional time-resolved velocity mapping (four-dimensional (4D) flow) covering the whole heart was performed during free breathing. The technique has been validated in vitro and in vivo.[64–67] More detailed parameters are reported in table 2. Controls underwent the same protocol.

Table 1.
Imaging parameters

Siemens 1.5 T MAGNETOM Aera			
Sequence parameters	**bSSFP CINE**	**2D Flow**	**4D Flow**
Flip angle [°]	70	20	8
TE/TR [ms]	1.2/2.7	2.7/4.9	3.5/5.6
Slice thickness [mm]	8	5	Not applicable
Slice gap [mm]	0	Not applicable	Not applicable
Reconstructed spatial resolution [mm^3]	1.2x1.2x8	1.6x1.6x5	3x3x3
Acquired temporal resolution [ms]	43	29	45
Reconstructed timephases	25	35	40
Gating method	Retrospective ECG	Retrospective ECG	Retrospective ECG
Velocity encoding (VENC) [cm/s]	Not applicable	200	100
Philips 1.5 T Achieva			
Sequence parameters	**bSSFP CINE**	**2D Flow**	**4D Flow**
Flip angle [°]	60	15	8
TE/TR [ms]	1.4/2.8	3.0/5.2	3.7/6.3
Slice thickness [mm]	8	6	Not applicable
Slice gap [mm]	0	Not applicable	Not applicable
Reconstructed spatial resolution [mm^3]	1.4x1.4x8	1.2x1.2x6	3x3x3
Acquired temporal resolution [ms]	47	29	50
Reconstructed timephases	30	35	40
Gating method	Retrospective ECG	Retrospective ECG	Retrospective ECG
Velocity encoding (VENC) [cm/s]	Not applicable	200	100

3.3 Image and Data Analysis

All MRI images were analysed using Segment software package (http://medviso.com) with an in-house developed module for 4D-flow analysis.[65] First-order phase background correction and phase unwrapping was performed.[68]

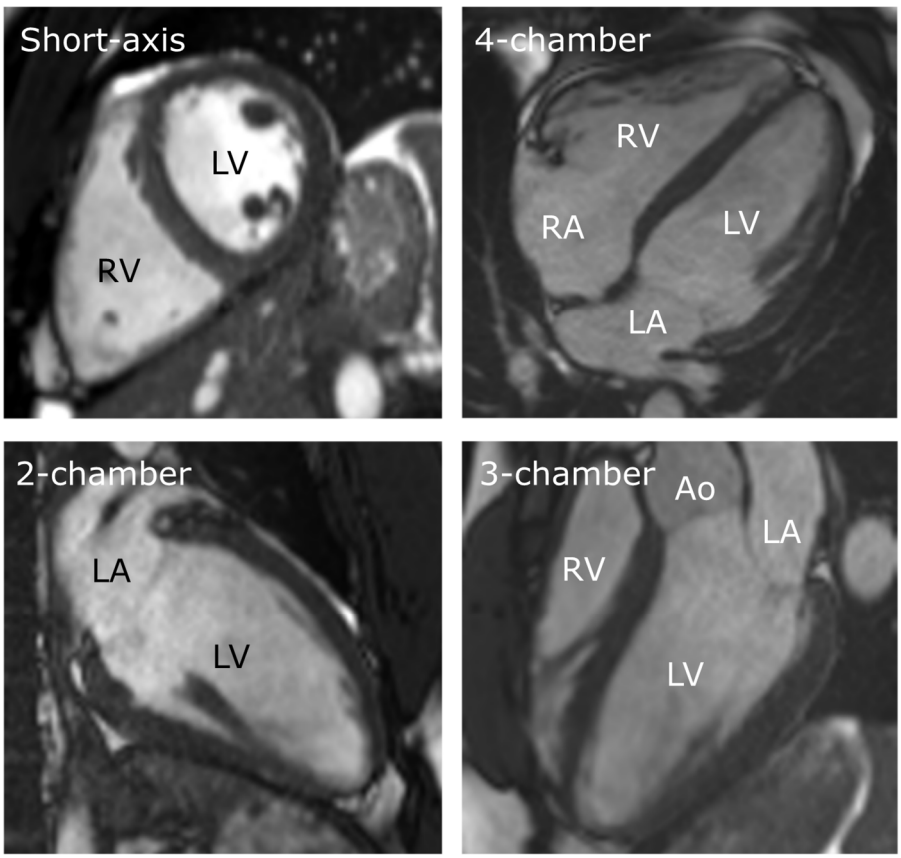

Figure 3.1
Typical images of the heart with magnetic resonance imaging. RV, right ventricle; LV, left ventricle; RA, right atrium; LA, left atrium; Ao, Aorta

Cine Imaging

Images from the whole cardiac cycle were acquired in a short-axis view and three long-axis views (Figure 3.1). Endocardial borders of the right and left ventricle were manually traced over the entire cardiac cycle to be transferred to the 4D-flow

dataset. The delineations were also used to derive end-diastolic and end-systolic volumes. Ventricular stroke volume was defined as end-diastolic volume – end-systolic volume. End-diastolic volume was set as the maximum volume and end-systolic volume as the minimum volume. Ejection fraction was defined as (stroke volume/end-diastolic volume)*100%. In paper IV, when analysing longitudinal pumping, end-diastole was set to the timeframe just before ventricular contraction and end-systole to the timeframe just before opening of the atrioventricular valves. Right and left atrium were delineated in ventricular end-diastolic and end-systolic timeframes for volume analysis. Delineations of the epicardium in short-axis images were used to calculate the longitudinal contribution to stroke volume in the LV. To acquire the tricuspid planes contribution to right ventricular stroke volume the largest end-systolic area of the right atrium just above and parallel to the tricuspid valve was delineated. Atrial reservoir volume was defined as maximum atrial volume – minimum atrial volume and atrial reservoir function was calculated by dividing atrial reservoir volume with left ventricular stroke volume. Atrial conduit volume was calculated by subtracting reservoir volume from left ventricular stroke volume.

Flow measurements

Two-dimensional flow measurements in the ascending aorta, pulmonary artery (paper I-IV), pulmonary veins (paper I) and superior caval vein (paper IV) was acquired for effective stroke volume and to assess aortopulmonary collateral flow (paper I), pulmonary regurgitation (paper II-IV) and inflow to the right atrium. Blood flow in the inferior caval vein was achieved by 4D flow in paper IV.

Lagrangian coherent structures

In the presence of pulmonary regurgitation there are two inflows to the right ventricle during diastole; one from the tricuspid valve and one from the pulmonary artery. To separate these flows Lagrangian coherent structures (LCS) was used in paper II. LCS defines boundaries of flow fields and can be shown as a line when observed in a two-dimensional plane. Analysis of LSC was obtained from 4D-flow data in the short-axis view at the time of peak diastolic kinetic energy.[69] In this way it was possible to distinguish how much the pulmonary regurgitation contributed to the kinetic energy in the ventricle.

Kinetic energy

Intraventricular kinetic energy was quantified in paper I and II. Endocardial delineations over the whole cardiac cycle in short-axis view were transferred to the 4D-flow dataset. Kinetic energy was calculated for each voxel as $KE = \frac{mv^2}{2}$

where m is mass of the blood in the voxel, calculated as the density (1.05 g/cm^3) multiplied by the volume of the voxel, and v is the velocity in the voxel. kinetic energy of all the voxels in the ventricles were added for each time frame of the cardiac cycle.

Kinetic energy was correlated to the anatomy by exporting velocity data and anatomical images to FourFlow software.

Kinetic energy was resampled in time to achieve the average kinetic energy over the cardiac cycle independent of individual heart rates to be able to compare groups.[70] Systolic and diastolic peak kinetic energy was defined as the highest value during systole or diastole respectively.

To be able to compare kinetic energy in patients with different heart sizes and stroke volumes kinetic energy was analysed not only in absolute values but also indexed to stroke volume (end-diastolic - end-systolic volume).

Hemodynamic forces

In paper III hemodynamic forces were analysed with an in-house developed module for 4D-flow analysis which has been validated in vivo and in vitro.[71] Time-resolved endocardial delineations were transferred to the 4D-flow data set. Based on the 4D-flow data the Navier-Stokes equation was used to calculate the pressure gradient (g) in N as $g = -\rho\frac{\partial v}{\partial t} - \rho(v \cdot \nabla v) + \mu\nabla^2 v$ where v is the velocity (m/s), ρ the density of blood (1.05 g/cm3) and μ the viscosity (4.0·10-3 Ns/m^2).

The hemodynamic force vectors were analysed in three dimensions and related to a reference system based in the anatomy of the heart (Figure 3.2). The AV-planes in the 2, 3 and 4-chamber views were used as reference and the apical-basal direction was defined as perpendicular to the AV-plane. The lateral-septal direction was defined as perpendicular to the apical basal direction and parallel to the 3-chamber long-axis image plane and the AV-plane. Finally, the inferior-anterior direction was defined as perpendicular to the other two directions. The transversal directions were renamed septal-freewall and diaphragm-RVOT (right ventricular outflow tract) in the right ventricle.

Hemodymamic force data were linearly interpolated in time to display the average force during the cardiac cycle in patients and controls and enable comparison. To facilitate comparison between forces regardless whether it was negative or positive

a root mean square (RMS) analysis was performed. RMS was calculated as $RMS = \sqrt{\frac{1}{N}\sum_{n=1}^{N} f_n^2}$ where *N* is the number of time frames in the cardiac cycle and *fn* is the force in the timeframe *n*. Forces were analysed in absolute values and indexed to volume to enable comparison between different heart sizes.

Ventricular motion

The lager right ventricular stroke volume compared to the left ventricular stroke volume in patients with pulmonary regurgitation causes the left ventricle to move more towards the right ventricle during systole then normal.[72,73] This might influence the measured hemodynamic forces quantified in paper III. To analyse the effect of ventricular motion on the hemodynamic forces the centre of the left and right ventricular volumes respectively were identified in end-diastole and the maximum distances in each force direction were calculated. The measured forces caused by ventricular motion could then be calculated and presented as proportion of the intraventricular hemodynamic forces.

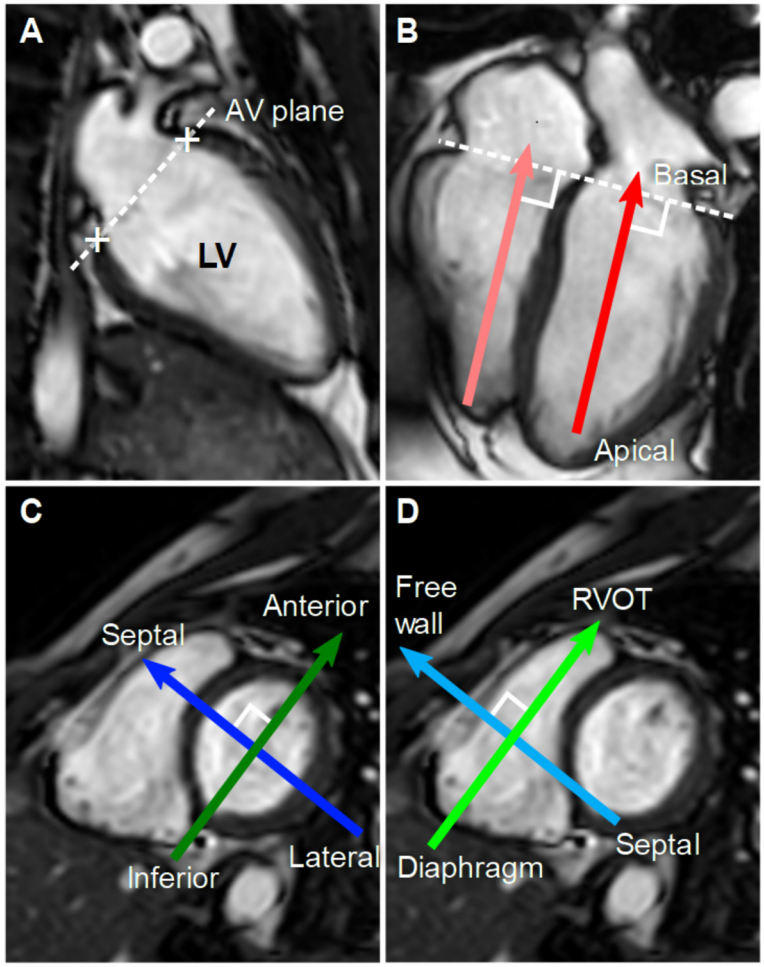

Figure 3.2 Spatial reference for hemodynamic forces.
A: the atrioventricular (AV) plane was defined in the two-, three-, and four-chamber views. B: the apical-basal direction was perpendicular to the AV plane. C: in the left ventricle the lateral-septal direction was parallel to the AV plane (perpendicular to the apical-basal direction) and parallel to the three-chamber long-axis image plane. The inferior-anterior direction was defined as perpendicular to both the apical-basal and lateral-septal planes. D:in the right ventricle (RV), the same directions were used but the transversal directions were renamed septal-freewall and diaphragm-RV outflow tract (RVOT).

Longitudinal function of the ventricles

The longitudinal function of the ventricles was in paper IV quantified using global longitudinal strain, mitral and tricuspid plane excursion (MAPSE and TAPSE respectively) and atrioventricular plane displacement (AVPD).

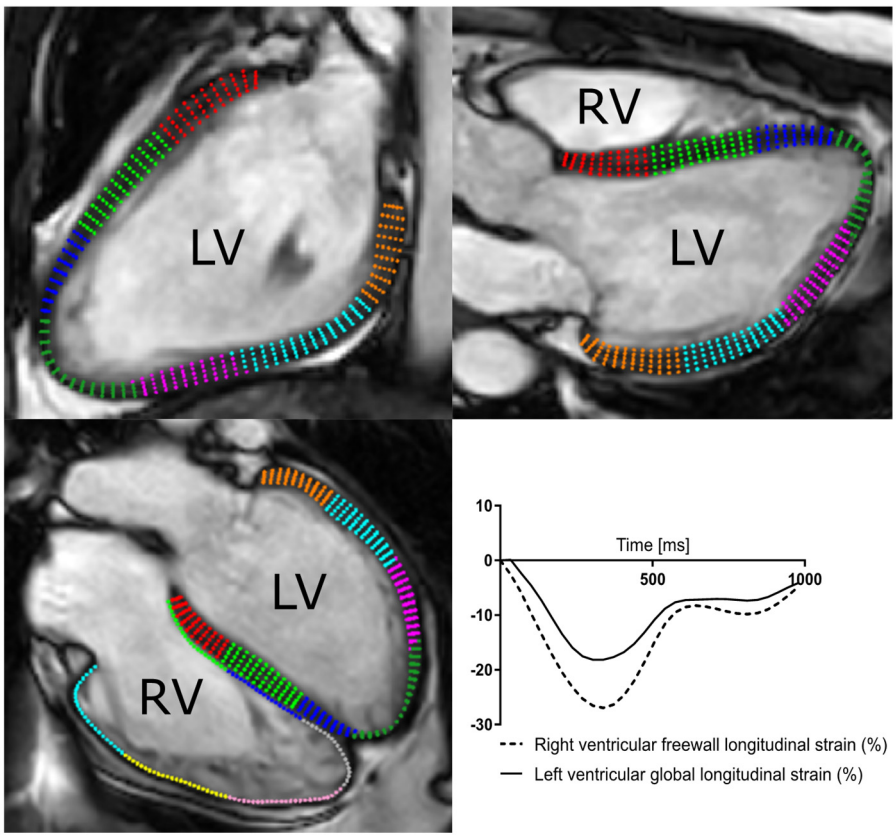

Figure 3.3 Global longitudinal strain
The myocardium was delineated in end-diastole and the relative change in muscle length during ventricular contraction was obtained using feature tracking.

Longitudinal strain was defined as the relative change in length of the myocardium during systole. Global longitudinal peak systolic strain using feature tracking was obtained from cine images where the myocardium was manually delineated in end-diastole. The delineations were automatically propagated throughout the cardiac cycle, with manual adjustments if necessary. The 2-, 3- and 4-chamber views were used for the left ventricle and the 4-chamber view for the right ventricle (Figure 3.3).

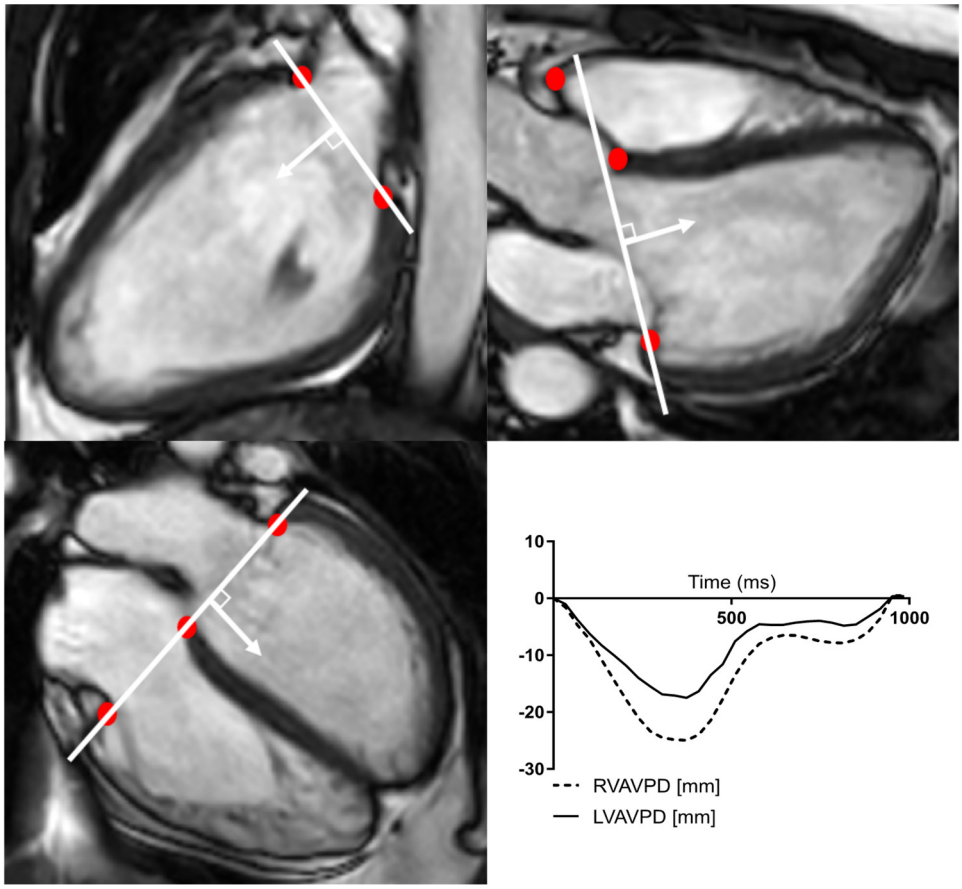

Figure 3.4 Atrioventricular plane displacement
The distance of the atrioventricular plane during ventricular contraction was semi-automatically quantified.

Atrioventricular plane displacement (AVPD) was defined as the distance of the atrioventricular plane towards the apex during systole measured perpendicular to the atrioventricular plane in end-diastole. Atrioventricular plane displacement was semi-automatically quantified in the 2-, 3- and 4-chamber views for the left ventricle and the 3- and 4-chamber views for the right ventricle (Figure 3.4).[74]

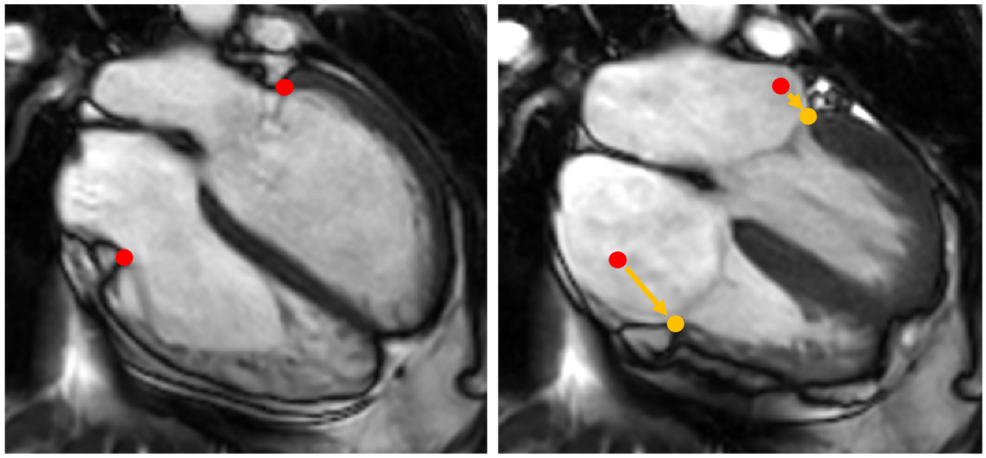

Figure 3.5 Mitral and tricuspid plane excursion
The distance between the lateral atrioventricular valve points in end-diastole and end-systole measured in the 4-chamber view.

Mitral and tricuspid plane excursion (MAPSE and TAPSE) was defined as the distance between the lateral atrioventricular valve points in end-diastole and end-systole measured in the 4-chamber view (Figure 3.5).

Longitudinal function was evaluated by calculating its contribution to stroke volume. For the left ventricle the mean of the two largest epicardial areas in short-axis views involving the AVPD was multiplied with the AVPD distance.[17] In the right ventricle this method would include the right ventricular outflow tract. Thus, to be able to differentiate the contribution to stroke volume caused by tricuspid plane excursion from the motion of the pulmonary valve, the right ventricular AVPD was multiplied with the largest area of the atrium in ventricular end-systole above and parallel to the tricuspid valve plane.

3.4 Statistical Analysis

Statistical analysis was performed using GraphPad (v6.04, La Jolla, CA; USA). Continuous variables were presented as mean and SD or median and range. Categorical variables were presented as absolute numbers or percentage. The Mann-Whitney U test or Student t-test were used to evaluate differences between patients and healthy volunteers. Wilcoxon rank test or paired t-test were used to assess differences between patients before and after intervention. Associations between variables were analysed by Spearman or Pearson correlation. Results with a p-value <0.05 were considered statistically significant. Correlation was defined as 0-0.19=very weak, 0.20-0.39=weak, 0.40-0.59=moderate, 0.60-0.79=strong and 0.80-

1.0=very strong. Cohen´s kappa was analysed for the relation of kinetic energy pattern and ventricular morphology (paper I) and systolic/diastolic peak kinetic energy and restrictive right ventricular physiology (paper II). Since the number of patients in paper I was small, statistical comparisons were not performed for differences between subgroups. Interobserver variability was assessed according to Bland-Altman with comparisons given in original units (mm, % or ml) as bias and standard deviations.

3.5 Exercise performance

Patients performed a maximal exercise test with continuous gas analysis (Carefusion, Oxycon Pro, Jaeger, Würzburg, Germany) on an ergometer (939 E, Monark, Vansbro, Sweden). The procedure was individualized with a 1-minute rest phase, 2-minute reference phase on no or low resistance before incremental workload until maximal exhaustion. To ensure maximal exertion, patients were encouraged to continue until respiratory exchange ratio was 1.1 or more. Peak oxygen uptake (VO_2) was registered and reported as ml/kg/min and as % of predicted value. Reference values for peak VO_2 were obtained from the SHIP study.[75] Twelve-lead ECG and blood saturation were recorded continuously, and blood pressure was measured at rest and every minute during exercise.

You never fail until you stop trying.

— Albert Einstein

4 Results and Comments

4.1 Kinetic energy

Study I and II

The kinetic energy of blood is defined as the work needed to accelerate a given mass of blood from rest to its current velocity. The looped shape anatomy of the heart has been proposed to help to conserve the momentum of the blood thereby decreasing the amount of work the heart must perform to accelerate the blood.[18] This may become more important during exercise when diastole is shorter and the stroke volume greater.[54,55] The external work needed to deliver a volume and pressure is divided into stroke work and kinetic energy. It is estimated that kinetic energy contributes to ~0.3% of the left ventricular external work and ~3% of the right ventricular work at rest.[53] During exercise, however, kinetic energy have been calculated to represent 3% of left ventricular work and 24% of the right. Intraventricular kinetic energy has shown to be altered in adult patients with heart failure, mitral regurgitation and cardiomyopathy but little is known about kinetic energy in congenital heart disease.[56–58] In study I and II, intraventricular kinetic energy was quantified for the first time during the entire cardiac cycle in patients with Fontan circulation and ToF.

The kinetic energy pattern during the cardiac cycle in Fontan patients was heterogenous because of patients' different ventricular morphologies and anatomy. Patients with right ventricular morphology had similar patterns as a right ventricle in the control group with a higher systolic than diastolic peak (systole/diastole>1). Patients with left ventricular morphology had patterns more like a healthy left ventricle, except for one patient with a ventricular septal defect and a small subaortic right ventricle (Figure 4.1). Cohen´s kappa for ventricular morphology and kinetic energy pattern was 1.0. The interventricular differences between the right ventricle working as a volume pump and the left ventricle as a pressure pump has been reported in other studies.[53,76]

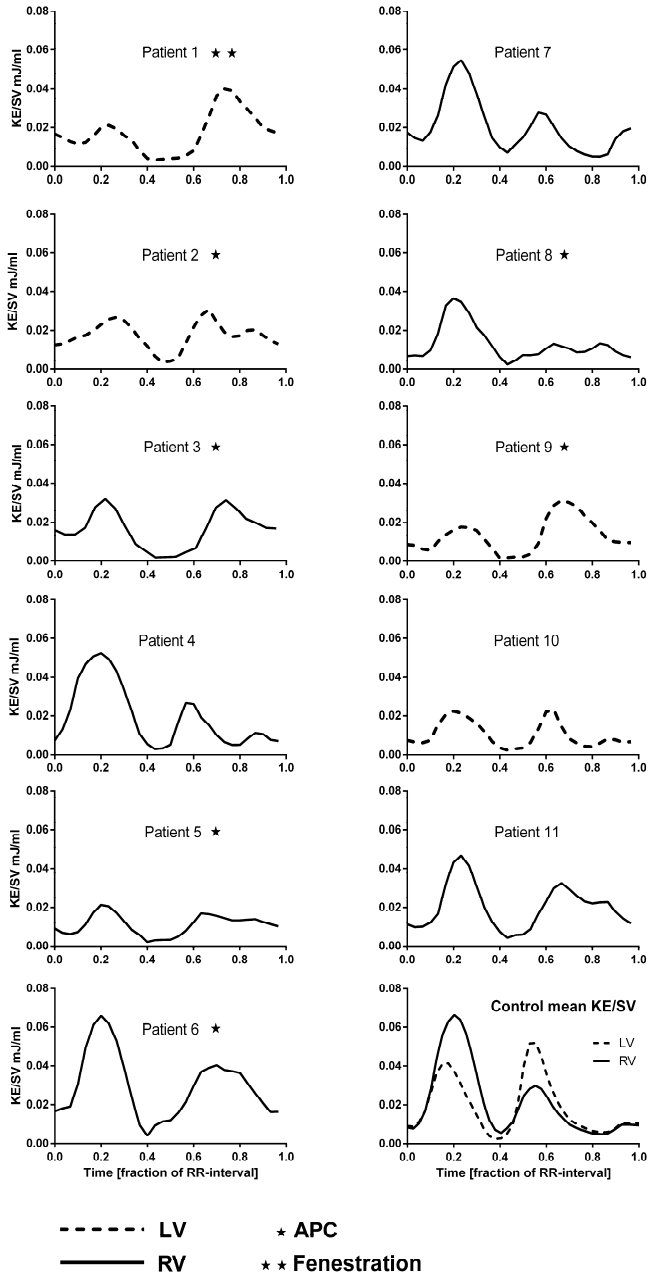

Figure 4.1 Kinetic energy in the ventricles of patients with Fontan circualtion during the cardiac cycle. Right ventricular (RV) morphology is shown in solid line. Left ventricular (LV) morphology is shown in broken line. The left column shows Fontan patients with complications. The right column shows patients with Fontan circulation without complications and a graph showing RV and LV of the control group. Patients with APC (aortopulmonary collaterals) are marked with a star. Patient 1 had a fenestrated extracardiac conduit which makes the assessment of APC difficult.

Thus, kinetic energy must be interpreted in relation to morphology and anatomy when compared to the normal values. This is reflected by the lack of difference in systolic kinetic energy between the whole group of Fontan patients compared to the left ventricle of controls. Dividing the patients into subgroups based on ventricular morphology revealed lower peak kinetic energy values in patients compared to controls in both groups (Figure 4.2). The number of patients in each group is small, why no statistical comparison was performed, but the numbers suggest that patients might have lower systolic kinetic energy in both right and left ventricles. The lower systolic kinetic energy might be explained by decreased ventricular filling leading to lower intraventricular flow but might also reflect a decreased systolic myocardial function. Diastolic kinetic energy was also lower in patients compared to controls irrespectively of the morphology. An explanation might be decreased preload, in contrast to adult heart failure patients who have backward failure and increased filling pressures resulting in increased diastolic kinetic energy.[57]

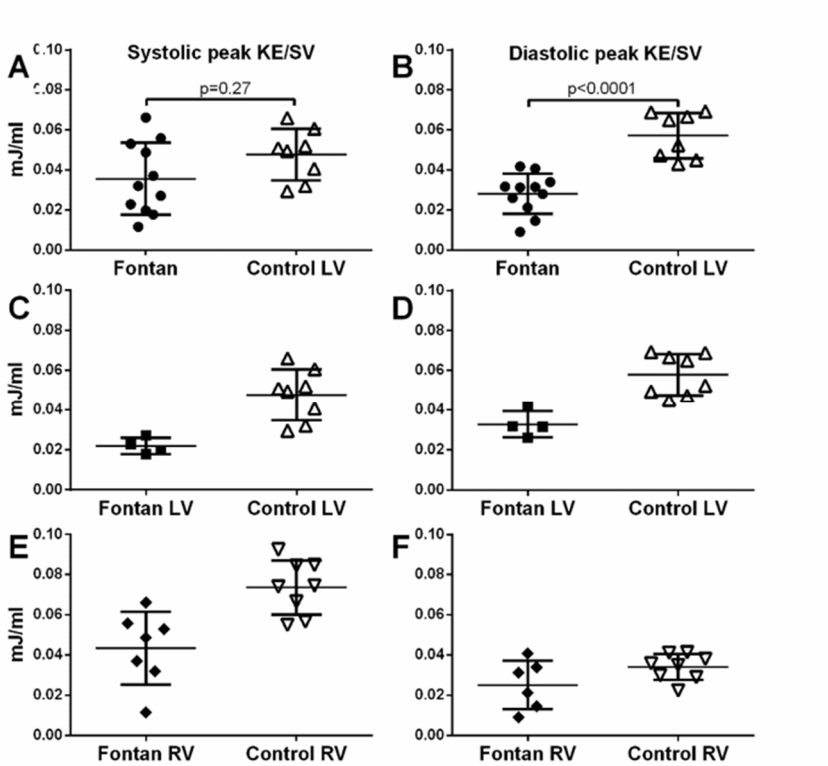

Figure 4.2 Kinetic energy (KE) indexed to stroke volume in patients with Fontan circulation
The left column shows peak KE during systole and the right column peak KE during diastole. A and B shows all Fontan patients and the left ventricle (LV) in the control group. C and D shows Fontan patients with LV morphology and the left ventricle in the control group. E and F shows Fontan patients with right ventricular (RV) morphology and the RV in the control group. Error bars show mean and SD.

In study I, three patients were examined after intervention (Table 4.1) and was found to have remarkably similar magnitude and basic pattern of kinetic energy, suggesting that kinetic energy pattern is specific to each individual (Figure 4.3). There were, however, some diastolic changes in two of the patients. In one patient (patient 6) this might be explained by closure of aortopulmonary collaterals resulting in lower inflow to the left atrium resulting in disappearance of the diastolic plateau. In the other patient (patient 4) the higher diastolic kinetic energy after surgery probably reflects an increase of aortopulmonary collaterals, which was diagnosed postoperatively. A diastolic plateau was also found in all Fontan patients with aortopulmonary collaterals which supports the hypothesis that diastolic kinetic energy might reflect left ventricular preload.

Table 4.1.
Characteristics and type of intervention in three patients who underwent cardiac magnetic resonance before and after intervention.

Subject	Diagnosis	Type of Fontan	Reason for intervention	Intervention
4	Hypoplastic right pulmonary artery, left isomerism, interrupted IVC, dextrocardia	Extracardiac	Pulmonary arteriovenous fistula. All liver drainage to one lung.	Extracardiac tunnel was converted to a Y-graft from the inferior vena cava to both pulmonary branches separately.
5	Hypoplastic aortic arch, CoA, VSD, DORV	Extracardiac	Stenosis of left pulmonary artery	Dilatation and stenting of left pulmonary artery
6	DORV Taussig Bing, unbalanced AVSD, PS, TAPVD, right isomerism	Extracardiac	APC	Coiling of collaterals

IVC, inferior vena cava; CoA, Coarctatio of aorta; VSD, ventricular septal defect; DORV, Double outlet right ventricle; AVSD, atrioventricular septal defect; PS, pulmonary stenosis; TAPVD, Total Anomalous Pulmonary Venous Drainage; APC, aortopulmonary collaterals

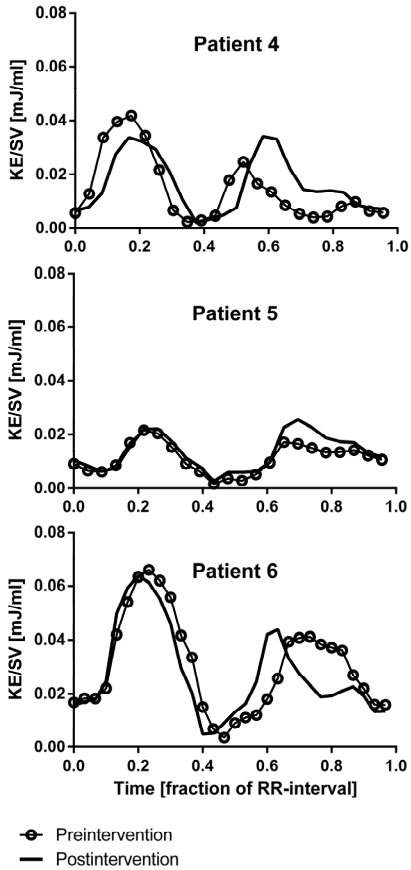

Figure 4.3 Kinetic energy (KE) indexed to stroke volume (SV) throughout the cardiac cycle in three patients before and after surgical or percutaneous intervention.
Details of the interven- tion are listed in Table 4.1. Heart rate (beats/minute) pre-intervention/ post-intervention was in patient 4: 103/87, patient 5: 85/83, patient 6: 63/80. The basic KE pattern for each patient is very alike at repeated examinations. A diastolic plateau might reflect aortopulmonary collaterals.

In study II, patients with rToF and pulmonary regurgitation, like Fontan patients, had decreased left ventricular systolic peak kinetic energy, even though they had preserved left ventricular ejection fraction (rToF 54±6% vs controls 57±5%, p=0.16) (Figure 4.4). Studies have shown that pulmonary regurgitation causes decreased left ventricular preload.[77,78] Therefore, at least part of the reason for decreased left ventricular systolic kinetic energy in patients with rToF and pulmonary regurgitation may be low preload as in Fontan patients. Another contributing factor could be septal dyssynchrony.[73,77]

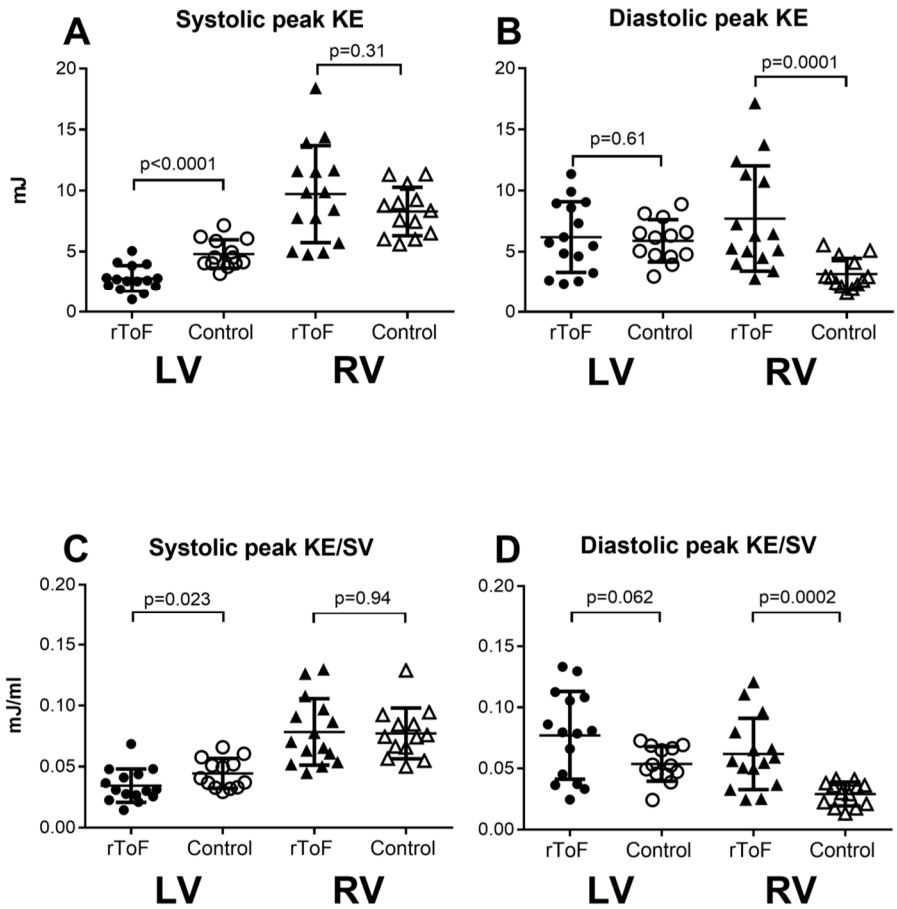

Figure 4.4 Peak kinetic energy in patients with repaired Tetralogy of Fallot and puplmonary regurgitation compared to controls
Comparison of peak kinetic energy (KE) (A, B) and peak KE indexed to stroke volume (SV) (C, D) between rToF patients and controls for both left ventricle (LV) and right ventricle (RV). A, C: Systolic KE and B, D diastolic KE. Bar and whiskers show mean ± SD. In the LV systolic KE in rToF is significantly lower than in controls. In the RV the diastolic KE is higher than in controls. The difference remains when indexed to SV.

In diastole there was no difference in left ventricular kinetic energy between patients with rToF and controls, which may be surprising since the preload is presumed to be low, as discussed above (Figure 4.4). However, patients with rToF and pulmonary regurgitation have been shown to have increased radial pumping which possibly compensate by increased suction raising the velocities.[73] This way patients with rToF differ from Fontan patients, since patients with rToF seem to have the capacity to compensate. The Fontan patients, on the other hand, either had right

ventricular morphology with low radial function or left ventricles that did not seem to be able to compensate for the low filling pressure.

There was no difference in systolic peak kinetic energy in the right ventricle in patients with rToF compared to controls, a result supported by an earlier study.[79] Increasing the volume passing a fixed right ventricular outflow tract would raise the velocities and cause a functional pressure drop between the right ventricle and the pulmonary artery, thereby also increasing the kinetic energy.[80] This since kinetic energy is defined by the mass and velocity squared. In patients with rToF and pulmonary regurgitation, however, the right ventricular outflow tract is wider than in controls. The lager stroke volume caused by the pulmonary regurgitation in patients do therefore not cause higher velocities. This could explain to the lack of difference in systolic peak KE between patients with rToF and pulmonary regurgitation and controls. After PVR 5/6 patients had decreased systolic peak kinetic energy in the right ventricle likely because the lower stroke volume. In one patient a widening patch in the right ventricular outflow tract was removed at the time of PVR. This resulted in a more restricted outflow tract causing the velocities to increase compared to before PVR.

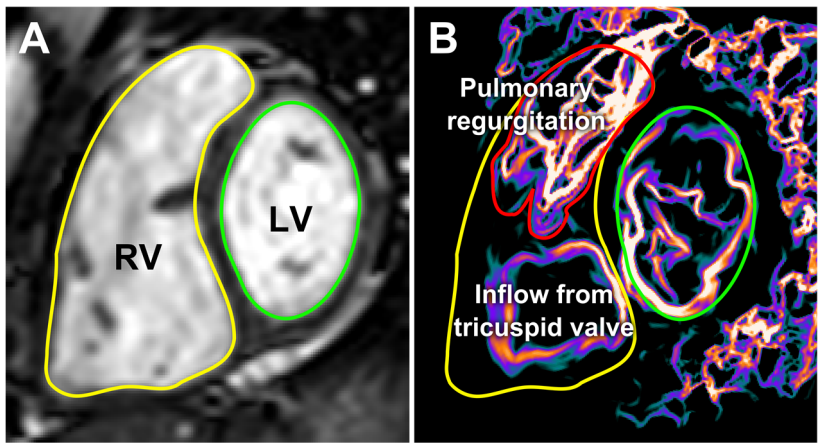

Figure 4.5. Differentiation of pulmonary regurgitation volume
A: SSFP short-axis view with the right ventricle (RV, outlined in yellow) and the left ventricle (LV) outlined in green. B: Same view with Lagrangian coherent structures (LCS) at the time of diastolic peak kinetic energy, visualizing the pulmonary regurgitation (outlined in red) and inflow to the right ventricle. LCS define boundaries of flow fields and thereby give a ring shape when a jet is directed towards or from the viewer in this image plane, e.g. the inflow to the right ventricle.

Right ventricular diastolic peak kinetic energy was increased in patients with pulmonary regurgitation compared to controls also after indexing for stroke volume (Figure 4.4). LCS was used to identify the region of pulmonary regurgitation at the time of diastolic peak kinetic energy (Figure 4.5). The regurgitation volume from the pulmonary artery contributed to major part of diastolic kinetic energy (64±17%)

and consequently right ventricular diastolic kinetic energy decreased after PVR (before PVR: 8.5±5.3 mJ; after PVR: 2.8±1.1 mJ, $p<0.05$).

The ratio between right ventricular peak systolic/peak diastolic kinetic energy was >1 in all patients with restrictive right ventricle, whereas 4/5 patients with non-restrictive physiology had ≤1 and 1/5 had a ratio of 1.1 (Cohen's kappa 0.84). No difference in the degree of pulmonary regurgitation was seen between the groups. The reason for higher ratio in restrictive ventricles might be that the lower compliance decreases the velocities of the inflow to the ventricle, whereas the compliant ventricle allows higher velocities.

Thus, kinetic energy seems to be specific for each individual heart and might be a useful non-invasive method of monitoring patients with congenital heart disease and detect signs of ventricular and circulatory dysfunction.

The results illustrate the complexity in evaluating kinetic energy. High kinetic energy could be good if it means that the blood keeps its energy but could also mean that there is a stenosis which will cause turbulence and hence energy loss. Low kinetic energy might represent the lack of stenosis but could also be a result of systolic dysfunction. Kinetic energy can nevertheless be a tool to better understand the pathophysiology of the failing heart.

4.2 Hemodynamic forces

Study III

During systole, when the ventricles contracts and ejects blood, the myocardium applies a force to accelerate the blood. For every action, there is an equal and opposite reaction, according to Newton's third law, which means that the blood also exerts a force on the myocardium. During late systole and diastole, the blood decelerates which leads to a counterforce with equal magnitude in the myocardium. Theoretically the hemodynamic forces ought to be aligned with the main blood flow directions for the heart to work as efficiently as possible and it has also been suggested that misalignment of intraventricular hemodynamic forces and blood flow may stimulate epigenetic mechanisms resulting in pathological cardiac remodelling [62,81]. Intraventricular hemodynamic forces are possible to quantify over the whole cardiac cycle in three dimensions using MRI. Hemodynamic forces are qualitatively similar in healthy controls and athletes, but altered in the left ventricle of heart failure patients with left bundle branch block and in dilated cardiomyopathy.[59–61] Patients with rTof and pulmonary regurgitation must accelerate a larger volume in the right ventricle and often have right bundle branch block which also might influence the intraventricular hemodynamic forces. Subsequently, study III aimed

to quantify the hemodynamic forces in the right and left ventricle in patients with rToF and pulmonary regurgitation to further understand the pathophysiology.

When calculating intraventricular forces, the translocation of the heart itself could be interfering.[72] When the whole heart moves, the blood volume also moves even if the blood is supposedly stagnant in relation to the heart. The ventricular motion was measured as the centre of volume variation during the cardiac cycle. In patients with rToF and pulmonary regurgitation the left ventricle moved more toward the septum/left ventricular outflow tract and inferiorly and the right ventricle moved more toward the free wall than in controls (Table 4.2). However, the gross cardiac motion did not influence the measurements of hemodynamic forces much, since it did not cause much acceleration of the blood and the magnitudes of the differences between the groups were considerably larger than the magnitudes caused by motion of the heart.

Table 4.2
Proportion of the calculated hemodynamic forces caused by the centre of volume motion of the left and right ventricles. Ventricular translocation affected the results to equal extent in patients and controls and the magnitudes of the differences between the groups were considerably larger than the magnitudes caused by motion of the heart.

Force direction %	Systole			Diastole		
Mean ± SD	rToF	Control	P-value	rToF	Control	P-value
Left ventricle						
Lateral-septal/LVOT	-8 ± 6	-7 ± 8	0.76	-11 ± 8	-9 ± 14	0.65
Inferior-anterior	-14 ± 16	-13 ± 16	0.68	-9 ± 12	-13 ± 20	0.63
Apical-basal	-1 ± 9	-4 ± 11	0.55	4 ± 9	4 ± 12	0.94
Right ventricle						
Septal-freewall	-5 ± 16	-3 ± 17	0.88	-15 ± 11	-15 ± 14	0.85
Diaphragm-RVOT	9 ± 7	10 ± 11	0.77	6 ± 11	-9 ± 11	0.0024
Apical-basal	0 ± 5	6 ± 16	0.0078	-6 ± 10	-9 ± 18	0.55

rToF, repaired Tetralogy of Fallot; LVOT, left ventricular outflow tract; RVOT, right ventricular outflow tract

In both patients and controls, the forces during early systole, were primarily directed toward the outflow tract and base of the heart in both the left and right ventricle reflecting the acceleration of blood in the ventricles toward the great arteries (Figure 4.6). In late systole the blood flow decelerates causing the forces to reverse. Early diastolic inflow of blood to the ventricles causes forces directed toward the apex and diaphragm, but forces are then reversed and oriented toward the base, reflecting deceleration of the inflow. In patients with pulmonary regurgitation there was also a decelerating force in the direction of the outflow tract throughout diastole.

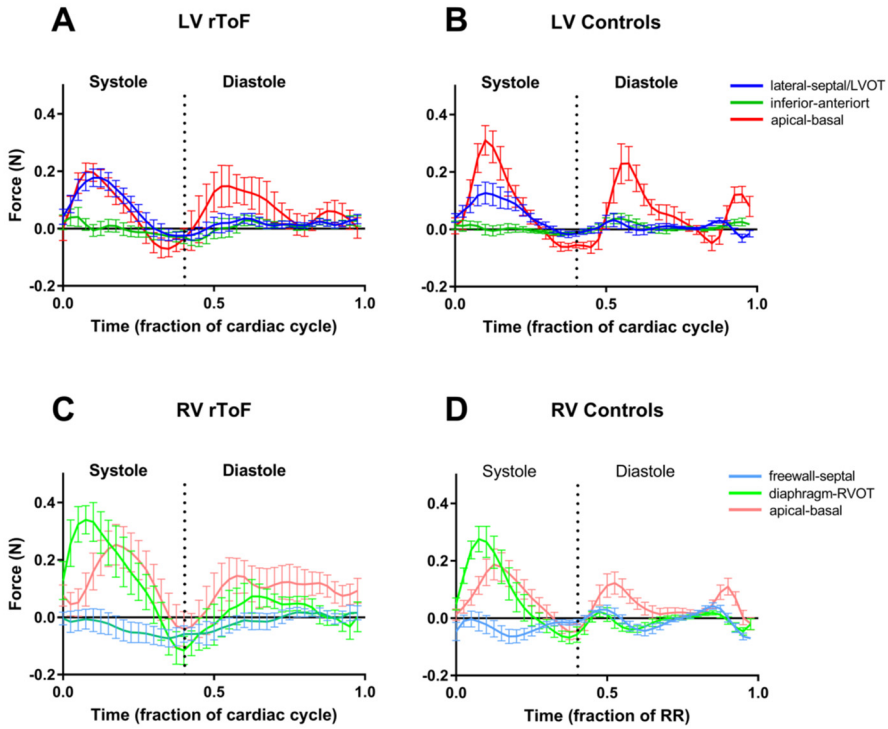

Figure 4.6. Mean hemodynamic forces with 95% confidence intervals during the cardiac cycle in patients with repaired Tetralogy of Fallot (rToF) and pulmonary regurgitation (A and C) and control subjects (B and D). A and B: data for the left ventricle (LV); C and D: data for the right ventricle (RV). In the LV, the hemodynamic forces are mainly directed toward the septum/LV outflow tract (LVOT) and the base when the blood is accelerated during systole and toward the base in diastole when blood entering the ventricle is decelerated. In the RV, the hemodynamic forces are mainly directed toward the RV outflow tract (RVOT) and base during systole reflecting the acceleration of the blood and during diastole toward the base because of the deceleration of the blood entering though the tricuspid valve, but in patients with rToF there is also a decelerating force toward the RVOT because of the pulmonary regurgitation volume.

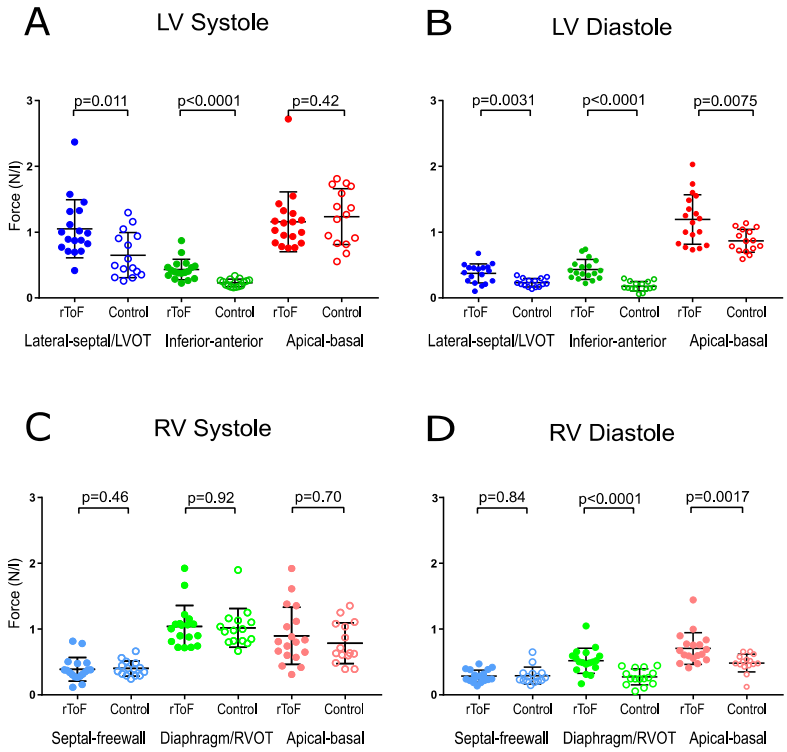

Figure 4.7. Root mean square (RMS) of hemodynamic forces indexed to ventricular volume in patients with repaired Tetralogy of Fallot (rToF) and pulmonary regurgitation (PR) and control subjects.
A and B: left ventricle (LV); C and D: right ventricle (RV). Systolic hemodynamic forces are shown on the left and diastolic on the right. Bar and whiskers show mean and SD. In the LV, patients with Tetralogy of Fallot and pulmonary regurgitation had higher hemodynamic forces in the lateral-septal/LV outflow tract (LVOT) direction and the inferior anterior direction, thus acting unaligned with the blood flow than control subjects in both systole and diastole. In the RV, there was no difference between patients with rToF and pulmonary regurgitation and control subjects in systole. However, in diastole, patients had higher decelerating forces on the blood flow from the pulmonary regurgitation (RV outflow tract (RVOT) direction) and tricuspid valve (basal direction).

To be able to compare hemodynamic forces regardless of them being positive or negative in relation to the defined direction, root mean square (RMS) analysis was performed.

In the left ventricle, both the inflow and outflow are in the longitudinal i.e. apical-basal direction. Compared to controls patients with rToF and pulmonary regurgitation had forces less aligned to the longitudinal direction of the left ventricle i.e. the main blood flow direction, and had higher transversal forces (Figure 4.7), suggesting a less efficient pumping and that there might be a substrate for pathological remodelling as discussed earlier. Left ventricular longitudinal forces in absolute numbers were lower in systole (0.13±0.035N) compared to controls

(0.18±0.062N; p=0.025), probably due to lower volumes caused by low preload. However, in diastole the indexed longitudinal force was increased compared to controls. This is in line with earlier studies showing lower preload and increased radial pumping in subjects with pulmonary regurgitation which would cause increased suction with unaffected diastolic kinetic energy as a result, as shown in paper II. [73,77]

In the right ventricle there was an increased force toward the base in diastole compared to controls. This force is a decelerating force on the inflowing blood from the tricuspid valve. The increase might partly be explained by decreased right ventricular longitudinal pumping causing the diastolic lengthening to reduce and filling of the ventricle resulting to a greater part than normal from radial pumping.[73] Contributing factors could also be higher central venous pressure than normal and restrictivity of the right ventricle. The higher force in patients compared to controls towards the outflow tract in diastole is, as mentioned before, a decelerating force because of the regurgitant volume from the pulmonary artery, thus not present in the control group. How much influence restrictive RV physiology has on the diastolic forces remains to be studied.

Table 4.3
Hemodynamic forces in patients with repaired Tetralogy of Fallot and pulmonary regurgitation before and after pulmonary valve replacement

Force direction Mean ± SD, n=8 N/l	Systole		Diastole	
	Before PVR	After PVR	Before PVR	After PVR
Left ventricle				
Lateral-septal/LVOT	1.11 ± 0.63	1.13 ± 0.43	0.40 ± 0.17	0.32 ± 0.13
Inferior-anterior	0.45 ± 0.22	0.39 ± 0.13	0.49 ± 0.18	0.43 ± 0.14
Apical-basal	1.28 ± 0.62	1.34 ± 0.32	1.06 ± 0.44	1.20 ± 0.44
Right ventricle				
Septal-freewall	0.35 ± 0.22	0.32 ± 0.14	0.30 ± 0.097	0.29 ± 0.093
Diaphragm-RVOT	1.12 ± 0.46 *	0.75 ± 0.17	0.58 ± 0.22 *	0.41 ± 0.11
Apical-basal	0.80 ± 0.50	0.65 ± 0.19	0.70 ± 0.33	0.64 ± 0.27

rToF, repaired Tetralogy of Fallot; LVOT, left ventricular outflow tract; RVOT, right ventricular outflow tract; PVR, pulmonary valve replacement
* p < 0.05, ** p<0.01, *** p<0.001

If the theory that misalignment of hemodynamic forces and main blood flow directions leads to pathological remodelling is correct, one of the major goals for treatment would be realignment of forces and flow. In this study we did not see any change in left ventricular forces after PVR. In the right ventricle, however, there was a decrease in forces in absence of the regurgitant volume, but they did not normalize in the direction diaphragm/right ventricular outflow tract (Table 4.3). In this direction patients after PVR had lower systolic forces and higher diastolic forces

than controls. The explanation for these disturbed forces in both ventricles after PVR is speculative but might be decreased myocardial systolic and diastolic function of the right ventricle or dyssynchrony. It might also indicate that the timing of surgery was not optimal but performed too late, however early postoperative sequelae might influence and longer follow up time is needed to see if forces will normalize in time.

4.3 Atrioventricular coupling

Study IV

It is debated when it is time to replace the valve in patients with ToF and pulmonary regurgitation.[28,36,82] Part of the reason may be that the methods commonly used to measure cardiac function are not sufficient or not properly understood. When the myocardium contracts it exerts a force on the intraventricular blood pool but the longitudinal ventricular function also pulls the atrioventricular (AV) plane toward the apex. This in turn causes a pressure gradient to aspirate blood into the atria from the caval and pulmonary veins. This coupling between the atria and the ventricles through longitudinal pumping can be assessed using MRI by strain, reflecting the myocardial contraction, AV-plane displacement and the resulting atrial volume changes and inflows of blood to the atria. The right and left ventricles also interact via their serial coupling and the common septal wall and position in the pericardial sac. It is important to understand what the different measurements of longitudinal function signify and what happens after PVR to use them properly in clinical practice for evaluation of patients both before and after PVR.

Right atrioventricular coupling

Myocardial strain has been used to assess ventricular function in patients with rToF and pulmonary regurgitation and has been shown to predict adverse outcome.[83,84] In study IV we found that patients with rToF and pulmonary regurgitation had lower global longitudinal strain of the right ventricular free wall than controls and it decreased further after PVR (Table 4.4). These results is in line with previous studies.[85–87] A decreased longitudinal contractility is however physiological due to atrioventricular coupling.[73,88] An almost constant outer volume requires that the same volume leaving the heart must enter almost simultaneously.[14,15] In presence of pulmonary regurgitation the right ventricle will receive blood from both the atrium and the pulmonary artery. During systole both volumes are ejected. If the pulmonary regurgitation is large the volume aspirated in to the right atrium in systole, which almost equals the ejected blood volume, could be more than the effective stroke volume (end-diastolic volume – end-systolic volume - regurgitant volume) and

would result in backward flow in the systemic veins during diastole. Thus, a decreased longitudinal function in patients with pulmonary regurgitation tells us that the pumping mechanics is changed but not necessarily that the ventricles capacity to contract has declined.

Our results also show that right ventricular longitudinal function was decreased in patients with rToF and pulmonary regurgitation compared to controls independent on the method used and did not correlate with ejection fraction (AVPD: r=0.22, p=0.50; right ventricular free wall strain: r=-0.34, p= 0.31) (Table 4.4).

Nevertheless, pulmonary regurgitation is likely not the only reason for decreased longitudinal function, since the decrease in longitudinal function was more than just to compensate for the pulmonary regurgitation volume. Compared to controls patients before PVR had decreased reservoir volume (atrial volume change in systole) and lower reservoir/conduit fraction in the right atrium (58 ± 8% vs 47±13%; p=0.036). The systolic caval blood flow showed very strong correlation to the right atrial reservoir volume as a verification of the measurements (Figure 4.8). These results are supported by other studies who showed decreased right atrial reservoir function in patients with rToF and pulmonary regurgitation.[78,89]

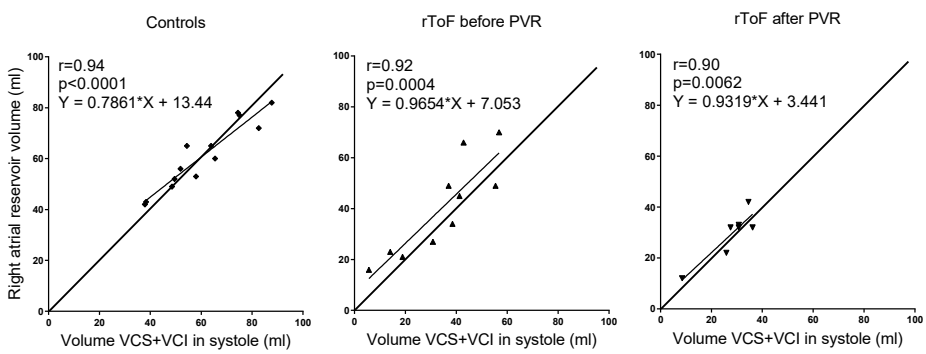

Figure 4.8. Correlation between right atrial reservoir volume and systolic venous return during systole. There was very strong correlation in both controls (n=12) and in patients (n=10) before and as well as after PVR, verifying the measurements of atrial reservoir volume.

The atrial reservoir volume also had strong correlation to the stroke volume caused by the systolic movement of the tricuspid plane in controls and patients before PVR, suggesting a clear atrioventricular coupling. (Figure 4.9). After PVR the atrioventricular coupling was lost which might be due to the recent pericardiotomy affecting the pumping mechanics. This may also explain why the longitudinal function did not increase after PVR in contrast to the results in an experimental study with percutaneous PVR.[77]

Table 4.4. Measurements of longitudinal function in patients with repaired Tetralogy of Fallot and pulmonary regurgitation before and after pulmonary vavle replacement and controls

Mean (SD)	Controls (n=15)	Patients with rToF before PVR (n=12)	Patients with rToF after PVR (n=12)
Age (years)	31 (7)	37 (13)**	38 (13)
Sex (male/female)	10/5	10/2	10/2
BSA (m^2)	1.9 (0.2)	2.0 (0.2)	2.0 (0.2)
Peak VO_2 (ml/min/kg)	-	25 (8)	29 (8)
Peak VO_2 (% of predicted)	-	80 (18)	87 (14)
Right ventricle			
RVEDV (ml)	192 (41)†††##	347 (65)***	240 (40)
RVEDV/BSA (ml/m^2)	101 (13)†††##	172 (24)***	118 (16)
RVESV (ml)	88 (23)†††###	195 (33)**	143 (30)
RVESV/BSA (ml/m^2)	46 (9)†††###	97 (11)**	70 (13)
RVSV (ml)	103 (19)†††	152 (43)***	97 (25)
RVEF (%)	55 (6)†††###	44 (6)	41 (7)
PRF (%)	-	44 (5)***	2 (1)
RV-AVPD (mm)	21.9 (1.9)†††###	11.4 (2.4)**	8.8 (2.7)
RV-AVPD (%)	22.9 (2.6)†††###	11.3 (2.3)**	8.8 (2.6)
TAPSE (mm)	28.6 (2.3)†††###	15.7 (3.6)*	14.5 (4.3)
RVFW GLS (%)	-26.6 (2.7)†††###	-22.0 (3.3)*	-18.7 (2.9)
Longitudinal contribution to RVSV (%)	58 (9)†††###	27 (7)	30 (11)
Left ventricle			
LVEDV (ml)	172 (36)	162 (31)	174 (38)
LVEDV/BSA (ml/m^2)	91 (14)†	80 (12)	86 (16)
LVESV (ml)	70 (17)	76 (16)	75 (21)
LVESV/BSA (ml/m^2)	37 (8)	38 (8)	37 (9)
LVSV (ml)	103 (23)	88 (25)*	100 (24)
LVEF (%)	60 (6)†	54 (7)	57 (7)
LV-AVPD (mm)	14.8 (1.8)†###	13.0 (2.8)**	11.6 (2.4)
LV-AVPD (%)	15.2 (2.5)##	13.5 (2.9)*	12.3 (2.2)
MAPSE (mm)	15.2 (2.2)	16.8 (3.4)	15.1 (3.6)
LV GLS (%)	-17.3 (1.7)	-16.5 (2.9)	-16.3 (2.5)
Longitudinal contribution to LVSV (%)	49 (8)	56 (11)**	48 (7)
Right atrium			
RAVmax/BSA (ml/m^2)	66 (11)††#	80 (29)*	72 (24)
RAVmin/BSA (ml/m^2)	37 (16)#	59 (24)	54 (20)
RAV Reservoir/BSA (ml/m^2)	32 (5)†††###	20 (9)	18 (6)
RAV Conduit/BSA (ml/m^2)	19 (4)†###	24 (7)*	30 (8)
Left atrium			
LAVmax/BSA (ml/m^2)	44 (6)	38 (12)	36 (9)
LAVmin/BSA (ml/m^2)	18 (4)	20 (8)	20 (8)
LAV Reservoir/ BSA (ml/m^2)	25 (4)††###	16 (9)	15 (7)
LAV Conduit/ BSA (ml/m^2)	29 (6)	27 (6)	30 (8)

rToF, repaired Tetralogy of Fallot; PVR, pulmonary valve replacement; HR, heart rate; BSA, Body Surface Area; RV, right ventricle; EDV, end-diastolic volume; ESV, end-systolic volume; SV, stroke volume; EF, ejection fraction; PRF, pulmonary regurgitation fraction; AVPD, atrioventricular plane displacement; TAPSE, tricuspid annular plane systolic excursion; FW, free wall; GLS, global longitudinal strain; LV, left ventricle; MAPSE, mitral annular plane systolic excursion; RAV, right atrial volume; LAV, left atrial volume.
† p < 0.05, †† p<0.01, ††† p<0.001 controls vs rToF before PVR
# p < 0.05, ## p<0.01, ### p<0.001 controls vs rToF after PVR
* p < 0.05, ** p<0.01, *** p<0.001 rToF before vs after PVR

Left atrioventricular coupling

The changes in pumping in patients with rToF was not just seen in the right ventricle. Left ventricular end-diastolic volume was decreased in patients with rToF and pulmonary regurgitation compared to controls (Table 4.4). Left ventricular longitudinal contraction, measured by global longitudinal strain, did not differ between controls and patients before PVR, similar to earlier results or after PVR (Table 4.4).[90] There was however a decrease in left ventricular atrioventricular plane displacement (AVPD) in patients before PVR compared to controls and AVPD decreased further after PVR (Table 4.4). These divergent results may indicate that the different measurement of longitudinal function cannot be used interchangeably.

The longitudinal contribution to stroke volume was numerically but not statistically higher (56±11%) in the presence of pulmonary regurgitation compared to controls (49±8%; p=0.059) (Table 4.4). Kopic *et al* showed increased longitudinal contribution to stroke volume in pigs with pulmonary regurgitation and the lack of statistical difference in our population could be the small number of patients.[77] In our study the left ventricular longitudinal contribution to stroke volume decreased after PVR (48±7%; p=0.006) to values similar to controls, supporting the results from the animal study where they also found a normalisation after PVR.

The interventricular interaction also plays a role in cardiac pumping and pulmonary regurgitation has been suggested to cause impaired filling of the left ventricle.[77,78] Our study shows lower left atrial reservoir volume in patients with pulmonary regurgitation compared to controls (Table 4.4) and since reservoir/conduit volume also is lower in patients with pulmonary regurgitation (39±11%) compared to controls (systole: 47±8%; p=0.027) the reason is presumably not just lower stroke volume. This result is in line with the results from study II and III showing that patients with rToF and pulmonary regurgitation have higher left ventricular diastolic hemodynamic forces, suggestively as a compensatory mechanism of the decreased preload, resulting in diastolic kinetic energy similar to controls.

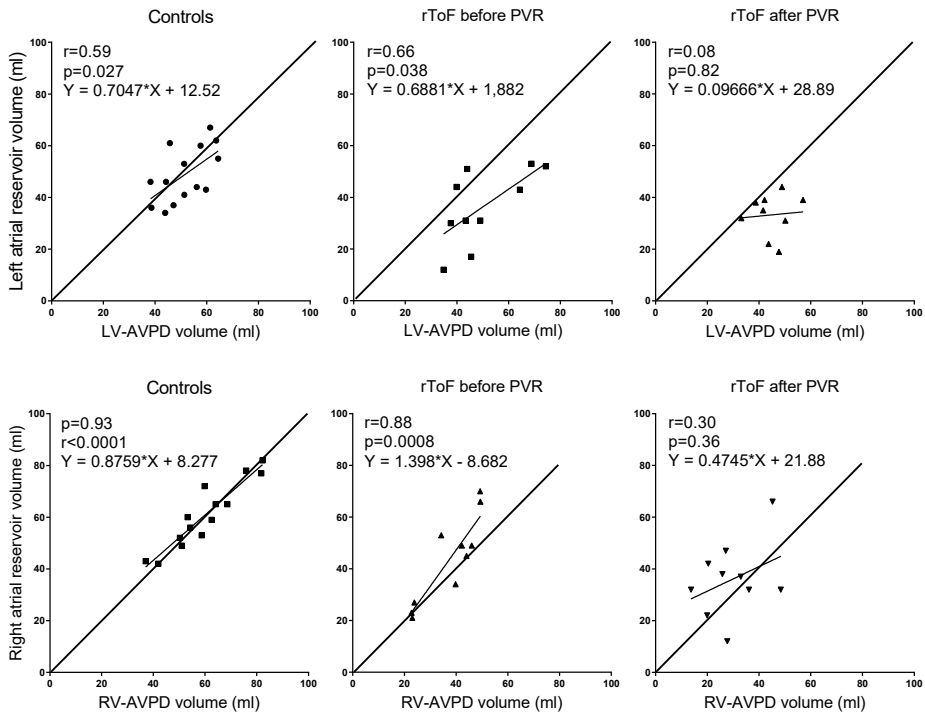

Figure 4.9.
Correlation between left right (upper panel) and right left (lower panel) atrial reservoir volume and the stroke volume produced by the right and the left atrioventricular plane displacement (RV-AVPD and LV-AVPD) in controls and, in patients before and after PVR.
The correlation seen in controls and in patients before PVR was not seen after PVR, showing that the atrioventricular coupling is lost after PVR.

After PVR left atrioventricular coupling was lost. The impact of intact pericardium on ventricular pumping has been addressed in another study suggesting increased stiffness of the atria. [91] Others however have reported increased compliance of the atria after pericardiotomy but these studies are often performed with open chests which might influence result.[92,93] Further, Voeller *et al* showed that in an experimental study there was no change in atrial stiffness 30 days after pericardiotomy. A study of adult patients who in childhood had undergone either atrial or arterial switch operation showed decreased left atrial reservoir function in both groups, although less after arterial switch, indicating that it is not just the scarring of the atrium that affects the function.[94] Thus, a hypothesis for the diminished atrioventricular coupling after PVR is that after pericardiotomy the pericardium loses its ability to maintain the normal pressure volume relations adding to the effect of atrial scarring. In theory these changes are energetically unfavourable as ventricular pumping will not fill the atria to the same degree but rather move

surrounding tissue. The loss of atrioventricular coupling after PVR makes assessment of longitudinal ventricular function difficult, which should be considered when evaluating treatment success.

4.4 Exercise performance

Study III and IV

Patients with rToF performed exercise test with gas analysis. In study III, where 6/15 patients were candidates for PVR . peak VO_2 was 30±10 ml/min/kg, equivalent to 86 ± 19 % of the predicted value [23,75], and in study IV where all 12 patients were planned for surgery peak VO_2 was 25±8 ml/min/kg (80 ± 18%), values similar to what other have reported.[23] After PVR there was no significant change in peak VO_2.(29±8 ml/ml; 87 ± 14%) indicating that the increased left ventricular preload did not have impact on this parameter, as also reported in another study.[86]

Correlation was analysed between peak VO_2 and pulmonary regurgitation volume, kinetic energy/stroke volume, ventricular volumes, stroke volume, ejection fraction, longitudinal strain and longitudinal contribution to stroke volume. In study III no correlation was found at all consistent with other studies except for right ventricular stroke volume that in other studies have shown a weak correlation.[95–97]

In study IV there was a strong positive correlation between peak VO_2 and left ventricular ejection fraction (r=0.62; p=0.041) and strong negative correlation between peak VO_2 and right ventricular end-systolic volume (r=-0.65; p=0.030). These correlations were not seen after PVR.

3. Conclusions

This thesis has investigated the cardiac function of patients with Fontan circulation and Tetralogy of Fallot using cardiac MRI. The major conclusions of each paper were:

Study I

Kinetic energy was to our knowledge quantified for the first time in patients with Fontan circulation. Kinetic energy is dependent on the morphology of the ventricle and the pattern over the cardiac cycle seems to be reproducible with repeated examinations. Kinetic energy might be a useful non-invasive method of monitoring patients with Fontan circulation to detect signs of circulatory dysfunction.

Study II

Quantification of kinetic energy over the entire cardiac cycle was to our knowledge performed for the first time. Kinetic energy is a potential marker for ventricular dysfunction and is disturbed in both the right and left ventricle in patients with Tetralogy of Fallot. Kinetic energy contributes to the understanding of the pathophysiology of pulmonary regurgitation.

Study III

Hemodynamic forces in both ventricles of patients with Tetralogy of Fallot and pulmonary regurgitation were quantified for the first time. Right ventricular hemodynamic forces are higher along the regurgitant flow in direction in the right ventricular outflow tract and that of the tricuspid inflow direction in patients with Tetralogy of Fallot and pulmonary regurgitation. Patients have less alignment of forces and the main blood flow directions in the left ventricle with normal ejection fraction. Forces are still altered compared to controls after PVR, suggesting that biventricular pumping does not normalize within a year after PVR.

Study IV

There was is a clear atrioventricular coupling with a strong relationship between systolic atrial inflow and ventricular longitudinal function in controls and patients before PVR. Within a year after PVR the atrioventricular coupling was deranged possibly because the loss of pericardial integrity. These changes are in theory energetically unfavourable. The impaired atrioventricular coupling makes it difficult to assess the ventricular function after surgery using measurements of longitudinal function.

4. Future Aspects

The first question that would be interesting to know the answer to is already put forward in study IV and that is if atrioventricular coupling improves in time after PVR and if this will affect the pumping mechanics, kinetic energy and hemodynamic forces.

Altered hemodynamic forces may contribute to increased wall stress which plays a role in ventricular remodelling [81]. Eriksson *et al* proposed that altered forces might result in a "vicious circle" with progression of pathological remodelling once started [61]. This could perhaps explain the difference in progression of right ventricular dilatation between patients with rToF and may give information about when it is time for PVR. In a more general perspective, hemodynamic forces might be used for optimizing cardiac resynchronisation and pacing but might also be applied in the context of preoperative planning.

Many patients with congenital heart defects adapt to a life with less physical activity [98] which might lead to a subjective overestimation of their physical capacity. Exercise can reveal a decreased cardiovascular function seemingly preserved at rest, why it is important to evaluate patients during stress [99]. The last years efforts in developing ways of examining patients in the MR scanner while performing physical exercise is now in a stage were studies on children and adults with congenital heart disease can be accomplished [100,101]. It would be interesting to see how cardiac pumping respond to physical exercise in patients with congenital heart defects. More specifically regarding patients with Fontan circulation the question is if they have different response to physical exercise regarding flow distribution to the lungs, aortopulmonary collateral flow, ventricular function, stroke volume and thereby cardiac output and if that might explain the difference in exercise capacity. In patients with Tetralogy of Fallot and pulmonary regurgitation it would be interesting to know how the leakage in the valve and pumping mechanics change with exercise, if that is related to exercise capacity and if it might predict the result of valve replacement.

The techniques are developing fast and 4D flow during exercise may be a possibility in the near future and this will open up for many interesting studies that might help us understand the pathophysiology of different congenital heart diseases.

Simulation of blood flow can be achieved by computational fluid dynamics and could make it possible to predict the result of planned interventions on an individual patient basis. This is a very interesting field that might help in guiding interventions especially in congenital heart disease.

For all that has been,
Thank you.

For all that is to come,
Yes!”

—Dag Hammarskjöld

5. Acknowledgements

I am very grateful to all people who helped me and inspired me over the years. If it were not for you this thesis will not have been written. There is not room to mention everyone, but I hope everyone feel my gratitude. Thank you all! A special gratitude to:

Marcus Carlsson, my main supervisor for all help, discussions, inspiration and for taking an old surgeon like me, showing that research can be a good substitute for surgery.

To my co-supervisors Petru Liuba for always being encouraging, Erik Hedström for offering help at all times and giving insightful comments on manuscripts and statistics and Johannes Töger for somehow always being able to program a solution to my questions.

The cardiac MR group in Lund, for creating an environment which gives the possibility to achieve a doctoral education out of the ordinary, not only in research but also in a wider perspective. It is unique. Håkan Arheden for fostering the special culture and for good discussions. Per Arvidsson for instant backing when I struggle with images. Sebastian Bidhult for endless patience in trying to teach me how computer programs works. Einar Heiberg and everyone at Medviso for their skills and will to help, always with good spirit. The wonderful technicians at the department of Clinical Physiology for MRI acquisitions.

My co-authors for their input and help with the papers in the thesis.

Soon-Ok Cha for showing me cardiac surgery and its beauty and constantly caring for the patients. Thanks also to all other colleagues and co-workers at the department of Thoracic Surgery in Örebro, for what I learned and for all the laughs over the years.

My former colleagues at the department of Pediatric Cardiac Surgery for sharing so much knowledge with me and for letting me be part of the fantastic work.

Eva Persson and Jonas Jögi for encouragement, good conversations and coping with by absent-mindedness lately.

Colleagues and staff at the department of Clinical Physiology for making it possible for research and clinical work go hand in hand and for all supportive words on the way.

My forever encouraging parents Ulla and Finn for all your love and support in every way through the years.

Jonas for love, for listening and for letting me share your life.

Erik and Emma for being the most wonderful kids anyone can wish for and giving the best hugs ever!

The studies were supported by grants from the Region of Skåne, Swedish Heart-lung Foundation, Swedish Medical Association, Lund University and Swedish Research Council.

6. References

1. Van Der Linde D, Konings EEM, Slager MA, Witsenburg M, Helbing WA, Takkenberg JJM, Roos-Hesselink JW. Birth prevalence of congenital heart disease worldwide: A systematic review and meta-analysis. *J Am Coll Cardiol*. 2011;58:2241–2247.
2. Bernier PL, Stefanescu A, Samoukovic G, Tchervenkov CI. The challenge of congenital heart disease worldwide: Epidemiologic and demographic facts. *Semin Thorac Cardiovasc Surg Pediatr Card Surg Annu*. 2010;13:26–34.
3. Carlgren L-E. The incidence of congenital heart disease in children born in Gothenburg 1941 1950. *Heart*. 2007;21:40–50.
4. Mandalenakis Z, Rosengren A, Skoglund K, Lappas G, Eriksson P, Dellborg M. Survivorship in children and young adults with congenital heart disease in Sweden. *JAMA Intern Med*. 2017;177:224–230.
5. Marelli AJ, Mackie AS, Ionescu-Ittu R, Rahme E, Pilote L. Congenital Heart Disease in the General Population Changing Prevalence and Age Distribution. 2007;Jan 16:163–72.
6. Liu Y, Chen S, Zu L, Black GC, Choy M, Li N, Keavney BD. Global birth prevalence of congenital heart defects 1970–2017: updated systematic review and meta-analysis of 260 studies. *Int J Epidemiol*. 2019;1–9.
7. Van Der Bom T, Bouma BJ, Meijboom FJ, Zwinderman AH, Mulder BJMM. The prevalence of adult congenital heart disease, results from a systematic review and evidence based calculation. *Am Heart J*. 2012;164:568–575.
8. Pfitzer C, Schmitt KRL, Ferentzi H, Bauer LRUMM, Berger F. Changing prevalence of severe congenital heart disease : Results from the National Register for Congenital Heart Defects in Germany. 2017;787–793.
9. Warnes CA, Williams RG, Bashore TM, Child JS, Connolly HM, Dearani JA, del Nido P, Fasules JW, Graham TP, Hijazi ZM, Hunt SA, King ME, Landzberg MJ, Miner PD, Radford MJ, Walsh EP, Webb GD, Smith SC, Jacobs AK, Adams CD, Anderson JL, Antman EM, Buller CE, Creager MA, Ettinger SM, Halperin JL, Krumholz HM, Kushner FG, Lytle BW, Nishimura RA, Page RL, Riegel B, Tarkington LG, Yancy CW. ACC/AHA 2008 Guidelines for the Management of Adults With Congenital Heart Disease. *J Am Coll Cardiol*. 2008;52:1890–1947.
10. Baumgartner H, Bonhoeffer P, De Groot NMS, De Haan F, Deanfield JE, Galie N, Gatzoulis MA, Gohlke-Baerwolf C, Kaemmerer H, Kilner P, Meijboom F, Mulder BJM, Oechslin E, Oliver JM, Serraf A, Szatmari A, Thaulow E, Vouhe PR, Walma E, Vahanian A, Auricchio A, Bax J, Ceconi C, Dean V, Filippatos G, Funck-Brentano C, Hobbs R, Kearney P, McDonagh T, Popescu BA, Reiner Z, Sechtem

U, Sirnes PA, Tendera M, Vardas P, Widimsky P, Swan L, Andreotti F, Beghetti M, Borggrefe M, Bozio A, Brecker S, Budts W, Hess J, Hirsch R, Jondeau G, Kokkonen J, Kozelj M, Kucukoglu S, Laan M, Lionis C, Metreveli I, Moons P, Pieper PG, Pilossoff V, Popelova J, Price S, Roos-Hesselink J, Uva MS, Tornos P, Trindade PT, Ukkonen H, Walker H, Webb GD, Westby J. ESC Guidelines for the management of grown-up congenital heart disease (new version 2010). *Eur Heart J*. 2010;31:2915–2957.

11. Cotts T, Khairy P, Opotowsky AR, John AS, Valente AM, Zaidi AN, Cook SC, Aboulhosn J, Ting JG, Gurvitz M, Landzberg MJ, Verstappen A, Kay J, Earing M, Franklin W, Kogon B, Broberg CS. Clinical research priorities in adult congenital heart disease. *Int J Cardiol*. 2014;171:351–360.
12. Widmaier E, Raff H, Strang K. Human Physiology, The Mechanisms of Body Function. 2018.
13. Hoit BD. Anatomy and Physiology of the Pericardium. Cardiol. Clin. 2017;35:481–490.
14. Bowman AW, Kovács SJ. Assessment and consequences of the constant-volume attribute of the four-chambered heart. *Am J Physiol Hear Circ Physiol*. 2003;285:H2027--H2033.
15. Carlsson M, Cain P, Holmqvist C, Stahlberg F, Lundback S, Arheden H. Total heart volume variation throughout the cardiac cycle in humans. *Am J Physiol Circ Physiol*. 2004;287:H243–H250.
16. Carlsson M, Ugander M, Mosén H, Buhre T, Arheden H. Atrioventricular plane displacement is the major contributor to left ventricular pumping in healthy adults, athletes, and patients with dilated cardiomyopathy. *Am J Physiol Circ Physiol*. 2007;292:H1452–H1459.
17. Carlsson M, Ugander M, Heiberg E, Arheden H. The quantitative relationship between longitudinal and radial function in left, right, and total heart pumping in humans. *Am J Physiol Circ Physiol*. 2007;293:H636–H644.
18. Kilner PJ, Yang GZ, Wilkes AJ, Mohiaddin RH, Firmin DN, Yacoub MH. Asymmetric redirection of flow through the heart. *Nature*. 2000;404:759–61.
19. 2017 SWEDCON Årsrapport. Nationellt register för medfödda hjärtsjukdomar Årsrapport 2017. 2017;
20. Bender HW, Fisher RD, Conkle DM, Martin CE, Graham TP. Selective Operative Treatment for Tetralogy of Fallot: Rationale and Results Eighty-one patients with tetralogy of Fallot malformations. *Ann Surg*. 1976;June:685–90.
21. Loomba RS, Buelow MW, Woods RK. Complete Repair of Tetralogy of Fallot in the Neonatal Versus Non-neonatal Period: A Meta-analysis. Pediatr. Cardiol. 2017;38:893–901.
22. Balasubramanya S, Zurakowski D, Borisuk M, Kaza AK, Emani SM, del Nido PJ, Baird CW. Right ventricular outflow tract reintervention after primary tetralogy of Fallot repair in neonates and young infants. *J Thorac Cardiovasc Surg*. 2018;155:726–734.
23. Kempny A, Dimopoulos K, Uebing A, Moceri P, Swan L, Gatzoulis MA, Diller G-P. Reference values for exercise limitations among adults with congenital heart

disease. Relation to activities of daily life--single centre experience and review of published data. *Eur Heart J*. 2012;33:1386–1396.

24. Harrison DA, Harris L, Siu SC, MacLoghlin CJ, Connelly MS, Webb GD, Downar E, McLaughlin PR, Williams WG. Sustained ventricular tachycardia in adult patients late after repair of tetralogy of Fallot. *J Am Coll Cardiol*. 1997;30:1368–1373.
25. Geva T. Indications and Timing of Pulmonary Valve Replacement After Tetralogy of Fallot Repair. *Pediatr Card Surg Annu*. 2006;9:11–22.
26. Bokma JP, Winter MM, Oosterhof T, Vliegen HW, van Dijk AP, Hazekamp MG, Koolbergen DR, Groenink M, Mulder BJ, Bouma BJ. Preoperative thresholds for mid-to-late haemodynamic and clinical outcomes after pulmonary valve replacement in tetralogy of Fallot. *Eur Heart J*. 2015;37:1–7.
27. Ferraz Cavalcanti PE, Sá MPBO, Santos CA, Esmeraldo IM, Escobar RR De, Menezes AM De, Azevedo OM De, Vasconcelos Silva FP De, Lins RFDA, Lima RDC. Pulmonary valve replacement after operative repair of Tetralogy of Fallot: Meta-analysis and meta-regression of 3,118 patients from 48 studies. *J Am Coll Cardiol*. 2013;62:2227–2243.
28. Alvarez-Fuente M, Garrido-Lestache E, Fernandez-Pineda L, Romera B, Sánchez I, Centella T, Abelleira C, Villagrá S, Tamariz R, Barrios E, Lamas MJ, Gomez R, Del Cerro MJ. Timing of Pulmonary Valve Replacement: How Much Can the Right Ventricle Dilate Before it Looses Its Remodeling Potential? *Pediatr Cardiol*. 2016;37:601–605.
29. Babu-Narayan S V., Diller GP, Gheta RR, Bastin AJ, Karonis T, Li W, Pennell DJ, Uemura H, Sethia B, Gatzoulis MA, Shore DF. Clinical outcomes of surgical pulmonary valve replacement after repair of tetralogy of fallot and potential prognostic value of preoperative cardiopulmonary exercise testing. *Circulation*. 2014;129:18–27.
30. Caldarone CA, McCrindle BW, Coles JG, Freedom RM, Williams WG, Van Arsdell GS, Caldarone CA, Webb G. Independent factors associated with longevity of prosthetic pulmonary valves and valved conduits. *J Thorac Cardiovasc Surg*. 2002;120:1022–1031.
31. Discigil B, Dearani JA, Puga FJ, Schaff H V, Hagler DJ, Warnes CA, Danielson GK. Late pulmonary valve replacement after repaired Tetralogy of Fallot. *J Thorac Cardiovasc Surg*. 2001;121:344–351.
32. Hallbergson A, Gauvreau K, Powell AJ, Geva T. Right ventricular remodeling after pulmonary valve replacement: early gains, late losses. *Ann Thorac Surg*. 2015;99:660–6.
33. Harrild DM, Berul CI, Cecchin F, Geva T, Gauvreau K, Pigula F, Walsh EP. Pulmonary valve replacement in tetralogy of Fallot. Impact on survival and ventricular tachycardia. *Circulation*. 2009;119:445–451.
34. Therrien J, Siu SC, Harris L, Dore A, Niwa K, Janousek J, Williams WG, Webb G, Gatzoulis MA. Impact of Pulmonary Valve Replacement on Arrhythmia Propensity Late After Repair of Tetralogy of Fallot. *Circulation*. 2001;103:2489–94.
35. Heng EL, Gatzoulis MA, Uebing A, Sethia B, Uemura H, Smith GC, Diller G-PP,

McCarthy KP, Ho SY, Li W, Wright P, Spadotto V, Kilner PJ, Oldershaw P, Pennell DJ, Shore DF, Babu-Narayan S V. Immediate and Midterm Cardiac Remodeling After Surgical Pulmonary Valve Replacement in Adults With Repaired Tetralogy of Fallot: A Prospective Cardiovascular Magnetic Resonance and Clinical Study. *Circulation*. 2017;136:1703–1713.

36. Greutmann M. Tetralogy of Fallot, pulmonary valve replacement, and right ventricular volumes: Are we chasing the right target? Eur. Heart J. 2016;37:836–839.
37. Kverneland LS, Kramer P, Ovroutski S. Five decades of the Fontan operation: A systematic review of international reports on outcomes after univentricular palliation. *Congenit Heart Dis*. 2018;13:181–193.
38. Fontan F, Baudet E. Surgical repair of tricuspid atresia. *Thorax*. 1971;26:240–8.
39. Chen S-CC, Nouri S, Glenn Pennington D, Pennington DG. Dysrhythmias after the modified Fontan procedure. *Pediatr Cardiol*. 1988;9:215–9.
40. Weber HS, Hellenbrand WE, Kleinman CS, Perlmutter RA, Rosenfeld LE. Predictors of rhythm disturbances and subsequent morbidity after the Fontan operation. *Am J Cardiol*. 2004;64:762–767.
41. Puga FJ, Chiavarelli M, Hagler DJ. Modifications of the Fontan operation applicable to patients with left atrioventricular valve atresia or single atrioventricular valve. *Circulation*. 1987;76:III53-60.
42. Pearl JM, Laks H, Stein DG, Drinkwater DC, George BL, Williams RG. Total cavopulmonary anastomosis versus conventional modified Fontan procedure. *Ann Thorac Surg*. 1991;52:189–196.
43. de Leval MR, Kilner P, Gewillig M, Bull C. Total cavopulmonary connection: a logical alternative to atriopulmonary connection for complex Fontan operations. Experimental studies and early clinical experience. *J Thorac Cardiovasc Surg*. 1988;96:682–95.
44. Laschinger JC, Ringel RE, Brenner JI, McLaughlin JS. Extracardiac total cavopulmonary connection. *Ann Thorac Surg*. 1992;54:371–373.
45. Marcelletti C, Corno A, Giannico S, Marino B. Inferior vena cava-pulmonary artery extracardiac conduit. A new form of right heart bypass. *J Thorac Cardiovasc Surg*. 1990;100:228–32.
46. Azakie A, Mccrindle BW, Arsdell G Van, Benson LN, Coles J, Hamilton R, Freedom RM, Williams WG. Extracardiac conduit versus lateral tunnel cavopulmonary connections at a single institution: Impact on outcomes. *J Thorac Cardiovasc Surg*. 2001;122:1219.
47. Dabal RJ, Kirklin JK, Kukreja M, Brown RN, Cleveland DC, Eddins MC, Lau Y. The modern Fontan operation shows no increase in mortality out to 20 years: a new paradigm. *J Thorac Cardiovasc Surg*. 2014;148:2517–2524.
48. d'Udekem Y, Iyengar AJ, Cochrane AD, Grigg LE, Ramsay JM, Wheaton GR, Penny DJ, Brizard CP. The Fontan Procedure: Contemporary Techniques Have Improved Long-Term Outcomes. *Circulation*. 2007;116:I-157-I-164.
49. Khairy P, Fernandes SM, Mayer JE, Triedman JK, Walsh EP, Lock JE, Landzberg MJ. Long-term survival, modes of death, and predictors of mortality in patients with

Fontan surgery. *Circulation*. 2008;117:85–92.

50. Brown JW, Ruzmetov M, Deschner BW, Rodefeld MD, Turrentine MW. Lateral Tunnel Fontan in the Current Era: Is It Still a Good Option? *Ann Thorac Surg*. 2010;89:556–563.
51. Gewillig M, Brown SC. The Fontan circulation after 45 years: update in physiology. *Heart*. 2016;102.
52. Gewillig M, Goldberg DJ. Failure of the fontan circulation. *Heart Fail Clin*. 2014;10:105–16.
53. Carlsson M, Heiberg E, Toger J, Arheden H. Quantification of left and right ventricular kinetic energy using four-dimensional intracardiac magnetic resonance imaging flow measurements. *Am J Physiol Heart Circ Physiol*. 2012;302:H893-900.
54. Kilner PJ, Henein MY, Gibson DG. Our tortuous heart in dynamic mode-an echocardiographic study of mitral flow and movement in exercising subjects. *Hear Vessel*. 1997;12:103–110.
55. Prec O, Katz N, Sennet L, Rosenman H, Fishman A, Hwang W. Determination of kinetic energy of the heart in man. *Am J Physiol*. 1949;159:483–491.
56. Al-Wakeel N, Fernandes JF, Amiri A, Siniawski H, Goubergrits L, Berger F, Kuehne T. Hemodynamic and Energetic Aspects of the Left Ventricle in Patients With Mitral Regurgitation Before and After Mitral Valve Surgery. *J Magn Reson Imaging*. 2015;42:1705–1712.
57. Kanski M, Arvidsson PM, Töger J, Borgquist R, Heiberg E, Carlsson M, Arheden H. Left ventricular fluid kinetic energy time curves in heart failure from cardiovascular magnetic resonance 4D flow data. *J Cardiovasc Magn Reson*. 2015;17.
58. Zajac J, Eriksson J, Dyverfeldt P, Bolger AF, Ebbers T, Carlhäll C-JJ. Turbulent kinetic energy in normal and myopathic left ventricles. *J Magn Reson Imaging*. 2015;41:1021–1029.
59. Arvidsson PM, Töger J, Carlsson M, Steding-Ehrenborg K, Pedrizzetti G, Heiberg E, Arheden H. Left and right ventricular hemodynamic forces in healthy volunteers and elite athletes assessed with 4D flow magnetic resonance imaging. *Am J Physiol - Hear Circ Physiol*. 2017;312:H314–H328.
60. Eriksson J, Zajac J, Alehagen U, Bolger AF, Ebbers T, Carlhäll CJ. Left ventricular hemodynamic forces as a marker of mechanical dyssynchrony in heart failure patients with left bundle branch block. *Sci Rep*. 2017;7:2971.
61. Eriksson J, Bolger AF, Ebbers T, Carlhäll CJ. Assessment of left ventricular hemodynamic forces in healthy subjects and patients with dilated cardiomyopathy using 4D flow MRI. *Physiol Rep*. 2016;4:e12685.
62. Pedrizzetti G, Martiniello AR, Bianchi V, D 'onofrio A, Caso P, Tonti G, D'Onofrio A, Caso P, Tonti G. Cardiac fluid dynamics anticipates heart adaptation. *J Biomech*. 2015;48:388–391.
63. Grosse-Wortmann L, Al-Otay A, Yoo SJ. Aortopulmonary collaterals after bidirectional cavopulmonary connection or fontan completion quantification with MRI. *Circ Cardiovasc Imaging*. 2009;2:219–225.

64. Kanski M, Töger J, Steding-Ehrenborg K, Xanthis CG, Markenroth Bloch K, Heiberg E, Carlsson M, Arheden H. Whole-heart 4D flow can be acquired with preserved quality without respiratory gating facilitating clinical use. *J Cardiovasc Magn Reson*. 2015;17:Q17.

65. Bock J, Töger J, Bidhult S, Markenroth Bloch K, Arvidsson P, Kanski M, Arheden H, Testud F, Greiser A, Heiberg E, Carlsson M. Validation and reproducibility of cardiovascular 4D-flow MRI from two vendors using 2 × 2 parallel imaging acceleration in pulsatile flow phantom and in vivo with and without respiratory gating. *Acta radiol*. 2019;60:327–337.

66. Töger J, Bidhult S, Revstedt J, Carlsson M, Arheden H, Heiberg E. Independent validation of four-dimensional flow MR velocities and vortex ring volume using particle imaging velocimetry and planar laser-Induced fluorescence. *Magn Reson Med*. 2016;75:1064–75.

67. Carlsson M, Töger J, Kanski M, Bloch KM, Ståhlberg F, Heiberg E, Arheden H. Quantification and visualization of cardiovascular 4D velocity mapping accelerated with parallel imaging or k-t BLAST: head to head comparison and validation at 1.5 T and 3 T. *J Cardiovasc Magn Reson*. 2011;13:55.

68. Busch J, Giese D, Kozerke S. Image-based background phase error correction in 4D flow MRI revisited. *J Magn Reson Imaging*. 2017;46:1516–1525.

69. Töger J, Kanski M, Carlsson M, Kovács SJ, Söderlind G, Arheden H, Heiberg E. Vortex Ring Formation in the Left Ventricle of the Heart: Analysis by 4D Flow MRI and Lagrangian Coherent Structures. *Ann Biomed Eng*. 2012;40:1–11.

70. Arvidsson PM, Töger J, Heiberg E, Carlsson M, Arheden H. Quantification of left and right atrial kinetic energy using four-dimensional intracardiac magnetic resonance imaging flow measurements. *J Appl Physiol*. 2013;114:1472–1481.

71. Töger J, Arvidsson PM, Bock J, Kanski M, Pedrizzetti G, Carlsson M, Arheden H, Heiberg E. Hemodynamic forces in the left and right ventricles of the human heart using 4D flow magnetic resonance imaging: Phantom validation, reproducibility, sensitivity to respiratory gating and free analysis software. *PLoS One*. 2018;13.

72. Carlsson M, Rosengren A, Ugander M, Ekelund U, Cain PA, Arheden H. Center of volume and total heart volume variation in healthy subjects and patients before and after coronary bypass surgery. *Clin Physiol Funct Imaging*. 2005;25:226–233.

73. Stephensen S, Steding-Ehrenborg K, Munkhammar P, Heiberg E, Arheden H, Carlsson M. The relationship between longitudinal, lateral, and septal contribution to stroke volume in patients with pulmonary regurgitation and healthy volunteers. *Am J Physiol Heart Circ Physiol*. 2014;306:H895-903.

74. Seemann F, Pahlm U, Steding-Ehrenborg K, Ostenfeld E, Erlinge D, Dubois-Rande J-L, Jensen SE, Atar D, Arheden H, Carlsson M, Heiberg E. Time-resolved tracking of the atrioventricular plane displacement in Cardiovascular Magnetic Resonance (CMR) images. *BMC Med Imaging*. 2017;17:19.

75. Gläser S, Koch B, Ittermann T, Schäper C, Dörr M, Felix SB, Völzke H, Ewert R, Hansen JE. Influence of age, sex, body size, smoking, and beta blockade on key gas exchange exercise parameters in an adult population. *Eur J Cardiovasc Prev Rehabil*. 2010;17:469–476.

76. Steding-Ehrenborg K, Arvidsson PM, Töger J, Rydberg M, Heiberg E, Carlsson M, Arheden H. Determinants of kinetic energy of blood flow in the four-chambered heart in athletes and sedentary controls. *Am J Physiol Heart Circ Physiol*. 2016;310:H113-22.

77. Kopic S, Stephensen SS, Heiberg E, Arheden H, Bonhoeffer P, Ersbøll M, Vejlstrup N, Søndergaard L, Carlsson M. Isolated pulmonary regurgitation causes decreased right ventricular longitudinal function and compensatory increased septal pumping in a porcine model. *Acta Physiol*. 2017;221:163–173.

78. Ylitalo P, Jokinen E, Lauerma K, Holmström M, Pitkänen-Argillander OM. Additional mechanism for left ventricular dysfunction: chronic pulmonary regurgitation decreases left ventricular preload in patients with tetralogy of Fallot. *Cardiol Young*. 2019;28:208–213.

79. Jeong D, Anagnostopoulos P V., Roldan-Alzate A, Srinivasan S, Schiebler ML, Wieben O, François CJ. Ventricular kinetic energy may provide a novel noninvasive way to assess ventricular performance in patients with repaired tetralogy of Fallot. *J Thorac Cardiovasc Surg*. 2014;149:1339–1347.

80. Rao PS, Awa S, Linde LM, Desk R, Williams L. Role of Kinetic Energy in Pulmonary Valvar Pressure Gradients. *Circulation*. 1973;48:65–73.

81. Mann DL. Basic mechanisms of left ventricular remodeling: the contribution of wall stress. *J Card Fail*. 2004;10:S202-6.

82. Shin YR, Jung JW, Kim NK, Choi JY, Kim YJ, Shin HJ, Park Y-H, Park HK. Factors associated with progression of right ventricular enlargement and dysfunction after repair of tetralogy of Fallot based on serial cardiac magnetic resonance imaging. *Eur J Cardiothorac Surg*. 2016;50:464–469.

83. Orwat S, Diller G-P, Kempny A, Radke R, Peters B, Kühne T, Boethig D, Gutberlet M, Dubowy K-O, Beerbaum P, Sarikouch S, Baumgartner H. Myocardial deformation parameters predict outcome in patients with repaired tetralogy of Fallot. *Heart*. 2016;102:209–215.

84. Kempny A, Diller G-P, Orwat S, Kaleschke G, Kerckhoff G, Bunck AC, Maintz D, Baumgartner H. Right ventricular-left ventricular interaction in adults with Tetralogy of Fallot: A combined cardiac magnetic resonance and echocardiographic speckle tracking study. *Int J Cardiol*. 2012;154:259–264.

85. Harrild DM, Marcus E, Hasan B, Alexander ME, Powell AJ, Geva T, McElhinney DB. Impact of transcatheter pulmonary valve replacement on biventricular strain and synchrony assessed by cardiac magnetic resonance feature tracking. *Circ Cardiovasc Interv*. 2013;6:680–687.

86. Ho JG, Schamberger MS, Hurwitz RA, Johnson TR, Sterrett LE, Ebenroth ES. The Effects of Pulmonary Valve Replacement for Severe Pulmonary Regurgitation on Exercise Capacity and Cardiac Function. *Pediatr Cardiol*. 2015;36:1194–203.

87. Scherptong RWC, Mollema SA, Blom NA, Kroft LJM, de Roos A, Vliegen HW, van der Wall EE, Bax JJ, Holman ER. Right ventricular peak systolic longitudinal strain is a sensitive marker for right ventricular deterioration in adult patients with tetralogy of fallot. *Int J Cardiovasc Imaging*. 2009;25:669–676.

88. Bowman AW, Kovács SJ. Left atrial conduit volume is generated by deviation from

the constant-volume state of the left heart: a combined MRI-echocardiographic study. *Am J Physiol Circ Physiol*. 2004;286:H2416–H2424.

89. Riesenkampff E, Mengelkamp L, Mueller M, Kropf S, Abdul-Khaliq H, Sarikouch S, Beerbaum P, Hetzer R, Steendijk P, Berger F, Kuehne T. Integrated analysis of atrioventricular interactions in tetralogy of Fallot. *Am J Physiol Heart Circ Physiol*. 2010;299:H364-71.

90. Balasubramanian S, Harrild DM, Kerur B, Marcus E, del Nido P, Geva T, Powell AJ. Impact of surgical pulmonary valve replacement on ventricular strain and synchrony in patients with repaired tetralogy of Fallot: a cardiovascular magnetic resonance feature tracking study. *J Cardiovasc Magn Reson*. 2018;20:37.

91. Riesenkampff E, Al-Wakeel N, Kropf S, Stamm C, Alexi-Meskishvili V, Berger F, Kuehne T. Surgery impacts right atrial function in tetralogy of Fallot. *J Thorac Cardiovasc Surg*. 2014;147:1306–1311.

92. Gaynor SL, Maniar HS, Prasad SM, Steendijk P, Moon MR. Reservoir and conduit function of right atrium: impact on right ventricular filling and cardiac output. *Am J Physiol Circ Physiol*. 2004;288:H2140–H2145.

93. Hoit BD, Shao Y, Gabel M, Walsh RA. Influence of pericardium on left atrial compliance and pulmonary venous flow. *Am J Physiol*. 1993;264:H1781-7.

94. Franzoso F, Wohlmuth C, Greutmann M, Kellenberger C, Oxenius A, Voser E. Atrial Function after the Atrial Switch Operation for Transposition of the Great Arteries: Comparison with Arterial Switch and Normals by Cardiovascular Magnetic Resonance. *Congenit Heart Dis*. 2016;11:426–436.

95. Mercer-Rosa L, Parnell A, Forfia PR, Yang W, Goldmuntz E, Kawut SM. Tricuspid Annular Plane Systolic Excursion in the Assessment of Right Ventricular Function in Children and Adolescents after Repair of Tetralogy of Fallot. *J Am Soc Echocardiogr*. 2013;26:1322–1329.

96. Kutty S, Shang Q, Joseph N, Kowallick JT, Schuster A, Steinmetz M, Danford DA, Beerbaum P, Sarikouch S. Abnormal right atrial performance in repaired tetralogy of Fallot: A CMR feature tracking analysis. *Int J Cardiol*. 2017;248:136–142.

97. Meadows J, Powell AJ, Geva T, Dorfman A, Gauvreau K, Rhodes J. Cardiac Magnetic Resonance Imaging Correlates of Exercise Capacity in Patients With Surgically Repaired Tetralogy of Fallot. *Am J Cardiol*. 2007;100:1446–1450.

98. Ko JM, White KS, Kovacs AH, Tecson KM, Apers S, Luyckx K, Thomet C, Budts W, Enomoto J, Sluman MA, Wang JK, Jackson JL, Khairy P, Cook SC, Subramanyan R, Alday L, Eriksen K, Dellborg M, Berghammer M, Johansson B, Mackie AS, Menahem S, Caruana M, Veldtman G, Soufi A, Fernandes SM, Callus E, Kutty S, Gandhi A, Moons P, Cedars AM. Physical Activity-Related Drivers of Perceived Health Status in Adults With Congenital Heart Disease. *Am J Cardiol*. 2018;122:1437–1442.

99. Jaijee S, Quinlan M, Tokarczuk P, Clemence M, Howard LSGE, Gibbs JSR, O'Regan DP. Exercise cardiac MRI unmasks right ventricular dysfunction in acute hypoxia and chronic pulmonary arterial hypertension. *Am J Physiol Circ Physiol*. 2018;315:H950–H957.

100. Steding-Ehrenborg K, Jablonowski R, Arvidsson PM, Carlsson M, Saltin B,

Arheden H. Moderate intensity supine exercise causes decreased cardiac volumes and increased outer volume variations: a cardiovascular magnetic resonance study. *J Cardiovasc Magn Reson*. 2013;15:96.

101. Claessen G, Schnell F, Bogaert J, Claeys M, Pattyn N, De Buck F, Dymarkowski S, Claus P, Carré F, Van Cleemput J, La Gerche A, Heidbuchel H, Gerche A La, Heidbuchel H. Exercise cardiac magnetic resonance to differentiate athlete's heart from structural heart disease. *Eur Heart J Cardiovasc Imaging*. 2018;19:1062–1070.

Printed by Media-Tryck, Lund 2019 NORDIC SWAN ECOLABEL 3041 0903

FACULTY OF MEDICINE

Department of Clinical Physiology

Lund University, Faculty of Medicine
Doctoral Dissertation Series 2019:56
ISBN 978-91-7619-785-1
ISSN 1652-8220